Vasoprotective activities of the adrenomedullin-RAMP2 system in endothelial cells

Xian Xian [a,b], Takayuki Sakurai Ph.D.[a], Akiko Kamiyoshi Ph.D.[a], Yuka Ichikawa-Shindo M.D., Ph.D.[a], Megumu Tanaka [a], Teruhide Koyama Ph.D.[a], Hisaka Kawate [a], Lei Yang Ph.D.[c], Tian Liu [a], Akira Imai M.D.[a], Liuyu Zhai M.D.[a], Kazutaka Hirabayashi M.D.[a], Kun Dai [a], Keiya Tanimura [a], Teng Liu [a], Nanqi Cui [a], Kyoko Igarashi Ph.D.[d], Akihiro Yamauchi Ph.D.[d], and Takayuki Shindo M.D., Ph.D. [a]

[a]Department of Cardiovascular Research, Shinshu University Graduate School of Medicine, Matsumoto, Japan
[b]Department of Pathogenic Biology, Hebei Medical University, Shijiazhuang, China
[c]Department of Epidemiology and Statistics, School of Public Health, Hebei Medical University, Shijiazhuang, China
[d]Japan Bio Products Co., Ltd., Tokyo, Japan

Abbreviated title:
Vasoprotection by endothelial AM-RAMP2 system

Key terms: Adrenomeullin (AM), Receptor activity-modifying protein (RAMP), Endothelial cells (ECs)

Number of Figure: 9**, Table:** 2, **Supplementary Figure:** 6

Address for correspondence
Takayuki Shindo, MD, PhD
Department of Cardiovascular Research,
Shinshu University Graduate School of Medicine
Asahi 3-1-1, Matsumoto, Nagano, 390-8621, Japan
Tel: +81-263-37-2578
Fax: +81-263-37-3437
Email: tshindo@shinshu-u.ac.jp

Disclosure statement: The authors have nothing to disclose

Abstract

Neointimal hyperplasia is the primary lesion underlying atherosclerosis and restenosis after coronary intervention. We previously described the essential angiogenic function of the adrenomedullin (AM)-receptor activity-modifying protein 2 (RAMP2) system. In the present study, we assessed the vasoprotective actions of the endogenous AM-RAMP2 system using a wire-induced vascular injury model. We found that neointima formation and vascular smooth muscle cell proliferation were enhanced in RAMP2+/- male mice. The injured vessels from RAMP2+/- mice showed greater macrophage infiltration, inflammatory cytokine expression and oxidative stress than vessels from wild-type mice, and less re-endothelialization. Following endothelial cell-specific RAMP2 deletion in drug-inducible endothelial cell-specific RAMP2-/- (DI-E-RAMP2-/-) male mice, we observed markedly greater neointima formation than in control mice. In addition, neointima formation following vessel injury was also enhanced in mice receiving bone marrow transplants from RAMP2+/- or DI-E-RAMP2-/- mice, indicating that bone marrow-derived cells contributed to the enhanced neointima formation. Finally, we found that the AM-RAMP2 system augmented proliferation and migration of endothelial progenitor cells. These results demonstrate that the AM-RAMP2 system exerts crucial vasoprotective effects following vascular injury and could be a novel therapeutic target for treatment of vascular diseases.

Abbreviations

AM: Adrenomedullin

RAMP: Receptor activity-modifying protein

ECs: Endothelial cells

VSMCs: Vascular smooth muscle cells

CLR: Calcitonin-receptor-like receptor

BMT: Bone marrow transplantation

EPCs: Endothelial progenitor cells

Introduction

Atherosclerosis is the leading cause of cardiovascular diseases. Both genetic and environmental components are associated with the development of atherosclerosis, but the primary cause is still a matter of considerable debate. Vascular endothelial cells (ECs) and vasoactive molecules play key roles in the maintenance of vascular homeostasis (1). ECs actively secrete a variety of bioactive molecules, including nitric oxide, natriuretic peptide, prostacyclin and adrenomedullin (AM). Originally identified as a vasodilating peptide isolated from human pheochromocytoma (2), AM is now known to be widely secreted from various organs and tissues, including ECs, and to be involved in a number of biological functions (3-10). Plasma levels of AM are elevated in patients with such cardiovascular diseases such as hypertension and congestive heart failure (11,12). There is also evidence that AM is associated with atherosclerosis. For example, AM production is decreased in the coronary circulation of patients with coronary artery disease (13), and AM levels in the coronary circulation after stent implantation could be a prognostic indicator for restenosis (14). In addition, we observed that vascular EC-specific AM-overexpressing mice showed resistance to neointimal hyperplasia and fatty streak formation (15).

AM is a member of the calcitonin superfamily and acts via a G protein-coupled seven transmembrane domain receptor (16), calcitonin-receptor-like receptor (CLR). The specificity of CLR for its ligands is determined by three receptor activity-modifying proteins, RAMP1, -2 and -3. We showed that homozygous RAMP2 knockout (RAMP2-/-) mice exhibit an embryonically lethal phenotype with abnormal vascular development that is nearly identical to that of AM-/- mice. Thus, deletion of RAMP2 almost entirely reproduces the major phenotypes of AM-/-, suggesting RAMP2 is specifically involved in the vascular function of AM (17). For that reason, we have been focusing on RAMP2 as an alternative therapeutic target for AM, since it may enable us to modulate the vascular functions of AM. To prove the importance of the vascular AM-RAMP2 system, we established vascular EC-specific RAMP2 conditional knockout mice (E-RAMP2-/-) (18). But although E-RAMP2-/- mice survive longer than RAMP2-/- mice, most died due to endothelial abnormalities and vascular leakage during the perinatal period. This highlights the importance of endothelial RAMP2 to the vascular AM-RAMP2 system.

In the present study, we examined the vasoprotective actions of the endogenous AM-RAMP2 system. Using a wire-induced vascular injury model, we analyzed the effect of RAMP2 deficiency on neointima formation in heterozygous RAMP2 knockout mice (RAMP2+/-). By utilizing drug-inducible endothelial cell-specific RAMP2−/− mice (DI-E-RAMP2−/−), we further analyzed the role of the vascular endothelial AM-RAMP2 system. We then tested whether inflammatory cell infiltration and reactive oxygen species (ROS) are involved in the development of neointimal hyperplasia, and because bone marrow-derived cells reportedly contribute to neointima formation, we also tested a bone marrow transplantation (BMT) model using these mice. Finally, we investigated the effects of the AM-RAMP2 system on the proliferation and migration of endothelial progenitor cells (EPCs).

Materials and methods

Animals

All of the animals used were C57BL/6J pure background male mice. RAMP2+/- mice were previously generated by our group (17). Tamoxifen drug-inducible vascular endothelial cell-specific RAMP2 knockout mice (DI-E-RAMP2-/-) were generated by crossbreeding mice expressing tamoxifen-inducible Cre-recombinase (Cre-ERT2) under the control of the vascular endothelial (VE)-cadherin promoter with floxed RAMP2 mice (RAMP2flox/flox). To induce RAMP2 gene-deletion in DI-E-RAMP2-/- mice, tamoxifen (Sigma-Aldrich, St. Louis, MO) was dissolved in corn oil (Sigma-Aldrich) to a concentration of 10 mg/ml, after which 1.5 mg was intraperitoneally injected into mice daily for 5 days. After 2 weeks of the induction of the gene-deletion, the expression of RAMP2 in the endothelial cells (ECs) decreased to less than 30% compared with the baseline level (Supplementary Figure 1). No significant difference was found in the serum AM level between control and DI-E-RAMP2-/- mice, or among the bone marrow transplantation (BMT) recipient mice (Supplementary Figure 2). We confirmed that the tamoxifen-treatment itself did not have an effect on the neointima formation (Supplementary Figure 3). Little toxicity was observed following the injection into WT, RAMP2 flox/flox, or Cre-ERT2 mice. Blood pressure was not different between the control and DI-E-RAMP2-/- mice (Supplementary Figure 4).

Mice were maintained under specific pathogen-free conditions in an environmentally controlled clean room at the Division of Laboratory Animal Research, Department of Life Science, Research Center for Human and Environmental Sciences, Shinshu University. All animal handling procedures were performed in accordance with protocols approved by the Ethics Committee of Institutional Animal Care and Use Committee and NIH guidelines (Guide for the care and use of laboratory animals).

Wire-induced vascular injury

Wire-induced injury of the left femoral artery and sham operation of the right femoral artery (no wire injury) were described previously by Sata et al. (19). Briefly, intraperitoneal injection of 2,2,2-tribromoethanol (240 mg/kg) was used for anesthesia during the operation. A straight spring wire (0.38 mm in diameter) was inserted into the

left femoral artery following the protocol described previously (20). The wire was left in place for 2 min to denude and dilate the artery. After removal of the wire, the proximal portion of the arterial branch was ligatured, and blood flow through the femoral artery was restored.

Histology and immunohistochemistry

The femoral arteries were excised from each mouse, fixed in 4% paraformaldehyde for 24-48 h and embedded in paraffin, after which the femoral arteries were cut into 4-μm-thick sections. The sections were stained with Elastica Van Gieson (EVG) or used for immunohistochemistry. For immunohistochemical analysis, arterial sections were incubated with rat anti-mouse CD31 (BD Biosciences, Franklin Lakes, NJ), mouse anti-human α-smooth muscle actin (Dako, Glostrup, Denmark), rat anti-mouse F4/80 (ThermoFisher Scientific, Waltham, MA), mouse anti-mouse 4-hydroxy-2-nonenal (4HNE) (NOF Corporation, Tokyo, Japan) or rabbit anti-mouse p67phox (MILLIPORE-UPSTATE, Billerica, MA). The sections were then stained with Alexa Fluor 488- or 568-conjugated anti-rabbit, anti-rat, or anti-mouse secondary antibody (ThermoFisher Scientific). To immunostain 4HNE, biotin-conjugated secondary antibodies were used. DAPI (Invitrogen, Carlsbad, CA) was used to stain the nuclei. Fluorescence was observed using a fluorescence microscope equipped with the appropriate filter sets (BZ-900, KEYENCE, Osaka, Japan).

Quantitative real-time RT-PCR analysis

Total RNA was extracted from tissues or cells using a PureLink™ RNA Mini Kit (Thermo Fisher Scientific) and subjected to reverse transcription using a High Capacity cDNA Reverse Transcription Kit (Applied Biosystems, Carlbad, CA). Quantitative real-time RT-PCR was carried out using an Applied Biosystems 7300 real time PCR System (Applied Biosystems) with SYBR green (Toyobo, Osaka, Japan) or Realtime PCR Master Mix (Toyobo) and TaqMan probe (MBL, Nagoya, Japan). The primers and probes used are listed in Tables 1 and 2. Values were normalized to GAPDH (Pre-Developed TaqMan assay reagents, Thermo Fisher Scientific). Sample numbers are shown in each figure legend.

Bone marrow transplantation (BMT)

Whole bone marrow cells were harvested from WT and RAMP2+/- mice or from DI-E-RAMP2-/- and control mice by flushing their femurs with physiological saline. The red blood cells were then lysed by incubation in ACK buffer (150 mmol/L NH4Cl, 10 mmol/L KHCO3, 0.1 mmol/L EDTA, pH 7.2) for 20 min at 0°C, as described previously (21). The remaining cells were washed 3 times with PBS and resuspended in 1 mL of PBS. Recipient mice (C57BL/6J background; purchased from Charles River Laboratories Japan, Inc.; male, 8-9 weeks old) were lethally irradiated with a total dose of 9 Gy of X-rays (MBR-155R2, Hitachi, Japan) and injected with bone marrow cells via the tail vein. We produced 4 types of BMT mice: WT to C57BL/6J ($BMT^{WT \rightarrow C57BL/6J}$) and RAMP2+/- to C57BL/6J ($BMT^{RAMP2+/- \rightarrow C57BL/6J}$), or control to C57BL/6J ($BMT^{Control \rightarrow C57BL/6J}$) and DI-E-RAMP2-/- to C57BL/6J ($BMT^{DI\text{-}E\text{-}RAMP2\text{-}/- \rightarrow C57BL/6J}$). After 8 weeks, all BMT mice underwent wire-induced vascular injury as described previously (21).

Bone marrow-derived EPC culture

Bone marrow-derived endothelial progenitor cells (EPCs) were cultured as described previously (22). Bone marrow cells were obtained from DI-E-RAMP2-/- or control mice. In DI-E-RAMP2-/-, the RAMP2 gene expression was significantly reduced compared with control (Supplementary Figure 5).

Mononuclear cells isolated from bone marrow cells (5×10^5/well) were cultured in 5% FBS/EBM-2 (Lonza, Basel, Switzerland) medium with supplements (SingleQuots Kit, Lonza) on vitronectin (BD Biosciences)-coated 12-well dishes and vitronectin-coated cover slips. After 28 days in culture, cells were incubated with acetylated low density lipoprotein labeled with 1,1'-dioctadecyl-3,3,3',3'-tetramethylindo-carbocyanine perchlorate (DiI-ac-LDL) (Thermo Fisher Scientific) for 5 h and then stained with FITC-conjugated lectin from Bandeiraea simplicifolia (FITC-BS-1-lectin) (Sigma-Aldrich). The dual-stained cells, considered to be EPCs, were counted in 12 randomly selected high-power fields under a fluorescence microscope.

Human EPC culture

Human (h)EPCs isolated from human cord blood were purchased from BioChain

(BioChain Institute, Inc., Newark, CA) and cultured in hEPC Growth Medium (BioChain) according to the supplier's protocol. The quality of hEPCs was checked based on uptake of DiI-ac-LDL, staining with FITC-BS-1-lectin and expression of CD34, which was assessed using real-time RT-PCR (data not shown). hEPCs with 6 to 8 passages were used in all experiments. Each individual experiment was repeated at least 3 times with different cell preparations.

Proliferation assay

hEPCs were cultured for 24 h in 96-well plates (2,500 cells/well) in hEPC Growth Medium, and then incubated with or without human AM (10^{-9}-10^{-7} M) for an additional 48 h. hEPC proliferation was then assessed using a Cell Counting Kit-8 (CCK-8, Sigma-Aldrich). As instructed in the manufacturer's protocol, 10 μl of CCK-8 solutions were added to each well of the plate. After incubation for 2.5 h, the absorbance at 450 nm was measured using a microplate reader.

Tube Formation Assay

In vitro tube formation assays were performed using Matrigel (BD Biosciences) according to the manufacturer's protocol. hEPCs were seeded onto a layer of Matrigel on plates and incubated for 48 h in hEPC medium with or without AM (10^{-7}M).

Statistical analysis

Values are expressed as means ± SE. Student's t test was used to determine significant differences between two groups. One-way ANOVA followed by Fisher's PLSD was used to determine significant differences between three or more groups. Values of $p< 0.05$ were considered significant.

Results

RAMP2+/- mice showed enhanced neointima formation

We initially used quantitative real-time PCR to analyze the relative gene expression of the AM-RAMP2 system in the femoral arteries of wild-type (WT) mice with (Injury) or without (Sham) wire-induced vascular injury. The expression of AM was significantly upregulated in the injured arteries of WT mice (Figure 1A). Thinking about its vasoprotective functions, upregulation of AM may reflect a compensatory response to the vascular injury.

In RAMP2+/- mice, expression of RAMP2 was reduced to half that in WT mice in both sham-operated (Figure 1B left) and wire-injured (Figure 1B right) arteries. The expression of CLR was also reduced in RAMP2+/- mice after wire injury. Elastica van Gieson (EVG) staining of the vascular lesions showed enhanced neointima formation in RAMP2+/- mice 28 days after vascular injury as compared to WT mice (Figure 1C). Quantitative analysis showed that neointimal areas and neointima/media (I/M) ratios were both significantly increased in RAMP2+/- mice (Figure 1D-E).

We next analyzed the cellular composition of the vascular lesions. Vascular re-endothelialization was assessed by immunostaining for the endothelial cell (EC) marker CD31, while vascular smooth muscle cell (VSMC) presentation was assessed by immunostaining for ⟨-smooth muscle actin (⟨-SMA). Consistent with earlier reports (19,23), neointimal lesions that formed after wire injury contained large numbers of VSMCs (Figure 1F). Moreover, within the neointima VSMCs were increased to a greater degree in RAMP2+/- than WT mice (Figure 1G), whereas vascular re-endothelialization was significantly decreased in RAMP2+/- as compared to WT mice (Figure 1F, G).

Inflammation was enhanced within vascular lesions in RAMP2+/- mice

Because inflammatory reactions are strongly associated with the progression of atherosclerosis and AM reportedly has anti-inflammatory effects, we assessed the inflammation within the vascular lesions. Immunostaining for F4/80 (Figure 2A) revealed that macrophages numbers in adventitial and neointimal areas were both significantly higher in RAMP2+/- than WT mice on day 28 after vascular injury (Figure 2B). At the same time, real-time PCR analysis revealed that expression levels of the

inflammation-related molecules CCR2, MCP-1, IL-6, and TNF-⟨, were all significantly increased in RAMP2+/- mice. Expression of the other inflammation-related molecules, including F4/80, CD68 and TGF®1 also tended to be higher in RAMP2+/- than WT mice (Figure 2C).

Oxidative stress was enhanced within vascular lesions in RAMP2+/- mice

Vascular inflammation is often accompanied by elevated oxidative stress, and AM stimulating pathways are known to cause an antioxidative effect (6). We therefore analyzed the oxidative stress level following wire-induced vascular injury. Immunostaining for p67phox, a cytosolic component of NADPH oxidase, was increased to a greater degree in the neointima of RAMP2+/- than WT mice (Figure 3A). Real-time PCR analysis also showed that, after wire injury, p67phox expression was significantly increased, while expression of endothelial nitric oxide synthase (eNOS) was slightly reduced in RAMP2+/- mice (Figure 3B). In both WT and RAMP2+/- arteries, immunostaining revealed the presence of 4-hydroxy-2-nonenal (4HNE), a product of lipid peroxidation, in the adventitia after wire injury. Within the neointimal lesions, however, RAMP2+/- arteries stained much more intensely for 4HNE than did WT arteries (Figure 3C).

Effect of vascular EC-specific RAMP2 deletion on neointima formation

To further clarify the involvement of ECs in the worsening of vascular lesions in RAMP2+/- mice, we utilized vascular EC-specific RAMP2 knockout mice (DI-E-RAMP2-/-). After inducing RAMP2 gene deletion for 1 week, femoral arteries were subjected to wire injury. Subsequent quantitative real-time PCR showed that AM expression was upregulated by wire injury in control arteries (Figure 4A). Compared with WT, DI-E-RAMP2-/- arteries showed significantly less RAMP2 expression in both sham-operated (Figure 4B left) and wire-injured (Figure 4B right) mice. Although we used EC-specific homozygous knockout mice, the reduction in gene expression was about 50% in control arteries, perhaps because other vascular cells also express RAMP2. AM expression was significantly unregulated in the DI-E-RAMP2-/- arteries, even without wire injury. This suggests that EC-specific RAMP2 deletion evokes the

compensatory upregulation of its ligand, AM, which is indicative of the particular importance of the endothelial AM-RAMP2 system. Interestingly, RAMP3 expression was also significantly upregulated in DI-E-RAMP2-/- arteries after wire injury (Figure 4B right), which suggests a complementary interaction between RAMP2 and RAMP3.

Using DI-E-RAMP2-/- mice, we investigated the effect of vascular EC-specific RAMP2-deficiency on neointima formation after wire-induced vascular injury. EVG staining revealed marked neointima formation in DI-E-RAMP2-/- mice 28 days after injury (Figure 4C), and quantitative analysis showed significant increases in both neointimal areas and I/M ratios in DI-E-RAMP2-/- mice (Figure 4D-E). Moreover, immunostaining for CD31 and ⟨-SMA, showed that vascular re-endothelialization following injury was significantly decreased in DI-E-RAMP2-/- mice, whereas VSMC proliferation within the neointima was markedly enhanced (Figure 4F-G).

Effect of vascular EC-specific RAMP2 deletion on inflammation and oxidative stress

When we immunostained arteries for F4/80 to detect the presence of macrophages (Figure 5A), we found that the numbers of macrophages in adventitial and neointimal areas were significantly higher in DI-E-RAMP2-/- than control mice on day 28 after vascular injury (Figure 5B). At the same time, levels of CCR2, MCP-1, IL-6 and TNF-⟨ expression were all significantly increased in DI-E-RAMP2-/- mice (Figure 5C).

Immunostaining revealed that levels p67phox were increased to a greater degree in the neointima of DI-E-RAMP2-/- than WT mice (Figure 6A). This was accompanied by significantly increased expression of p67phox (Figure 6B). In addition, levels of 4HNE were also higher in wire-injured arteries from DI-E-RAMP2-/- mice than WT mice, particularly in the neointima (Figure 6C).

Effect of RAMP2 in bone marrow-derived cells on neointima formation

It has been suggested that bone marrow cells participate in neointima formation after vascular injury (23-25). To assess the effect of RAMP-deficiency in bone marrow on the neointima formation seen in RAMP2+/- mice, we performed bone marrow transplantation (BMT) ($BMT^{WT\rightarrow C57BL/6J}$, $BMT^{RAMP2+/-\rightarrow C57BL/6J}$) and evaluated

neointima formation following wire-induced injury. Quantitative analysis showed that the neointimal areas, medial areas and I/M ratios were all significantly larger in $BMT^{RAMP2+/-\rightarrow C57BL/6J}$ than $BMT^{WT\rightarrow C57BL/6J}$ mice (Figure 7A-B). Immunostaining for CD31 and ⟨-SMA showed that vascular re-endothelialization was significantly reduced and neointimal VSMC proliferation was significantly upregulated in $BMT^{RAMP2+/-\rightarrow C57BL/6J}$ mice (Figure 7C-D).

To assess the role of bone marrow-derived cells in the enhanced neointima formation seen in DI-E-RAMP2-/- mice, we also evaluated neointima formation following wire-induced injury in $BMT^{control\rightarrow C57BL/6J}$ and $BMT^{DI\text{-}E\text{-}RAMP2\text{-}/\text{-}\rightarrow C57BL/6J}$ mice. We observed that I/M ratios were significantly increased in $BMT^{DI\text{-}E\text{-}RAMP2\text{-}/\text{-}\rightarrow C57BL/6J}$ mice (Figure 8A-B). In addition, vascular re-endothelialization was significantly reduced while neointimal VSMC proliferation was significantly increased in $BMT^{DI\text{-}E\text{-}RAMP2\text{-}/\text{-}\rightarrow C57BL/6J}$ mice (Figure 8C-D).

Effects of RAMP2 on EPC proliferation and tube formation

We also examined the function of the AM-RAMP2 system in endothelial progenitor cells (EPCs) *in vitro*. EPCs were initially cultured from bone marrow from control and DI-E-RAMP2-/- mice, and Dil-Ac-LDL uptake and staining for BS-1 lectin were analyzed. After 28 days of culture, there were fewer Dil-Ac-LDL and BS-lection double-positive EPCs in DI-E-RAMP2-/- than control mice (Figure 9A, B). RT-PCR analysis of blood-derived hEPCs showed expression of AM, RAMP2 and CLR (Figure 9C). WST cell proliferation assays showed that AM administration significantly enhanced hEPC proliferation (Figure 9D), while capillary formation assays showed that AM significantly enhanced capillary formation on Matrigel (Figure 9E, F).

Discussion

Atherosclerosis is the leading cause of death worldwide. Narrowing of arterial lumens due to atherosclerotic plaque development or plaque rupture can interrupt normal blood flow, leading to myocardial infarction or stroke. Percutaneous interventions, including balloon angioplasty and stenting have been used to treat occlusive vascular diseases; however, restenosis remains a major cause of failure of endovascular treatments for atherosclerosis. Precise understanding of the processes underlying atherosclerosis and restenosis will help to identify new biomarkers and targets for novel treatments. We and others have suggested that AM could be one such candidate. Although AM is secreted from various organs and tissues, it is mainly produced by vascular ECs (26) and, to a lesser extent, VSMCs (27). AM initially attracted attention as a vasoactive peptide that induced vasodilation and lowered blood pressure (2). We reported that AM knockout (AM-/-) mice die in utero due to vascular structural abnormalities (28), which indicates that AM is indispensable for proper vascular development. We also observed that blood vessel-specific AM overexpression makes mice resistant to neointimal hyperplasia induced by periarterial cuff placement (15). AM stimulates EC proliferation and inhibits EC apoptosis (19,29) as well as the migration and proliferation of VSMCs (30). Consistent with those findings, hypercholesterolemia-induced fatty streak formation was reduced in apolipoprotein E knockout mice (ApoE-/-) crossed with blood vessel-specific AM transgenic mice (15). Therefore, in addition to its angiogenic function, AM appears to possess vasoprotective actions against various injuries.

Because of the wide range of its bioactivity, AM has been attracting attention for its potential clinical application. But like other bioactive endogenous peptides, the clinical applicability of AM has limitations, the most obvious of which is its very short half-life in the blood, which makes its use impractical for treatment of chronic diseases. AM and its family peptides partially share the same receptor, CLR; ligand specificity is determined by the RAMPs. We showed that homozygous RAMP2 knockout (RAMP2-/-) mice exhibit an embryonically lethal phenotype with abnormal vascular development that is essentially identical to the AM-/- phenotype (17). This suggests RAMP2, in particular, could be a therapeutic target through which to manipulate the vascular function of AM. We have therefore worked to clarify the pathophysiological functions

of the AM-RAMP2 system by generating and utilizing a series of genetically engineered mice.

In an earlier study, we showed that the angiogenic function of AM is RAMP2-dependent and speculated that RAMP2 also regulates the vasoprotective functions of AM (18). In the present study, we utilized RAMP2+/- and drug-inducible EC-specific RAMP2 knockout mice (DI-E-RAMP2-/-) in a wire injury model to evaluate the function of the endogenous AM-RAMP2 system. Our findings are as follows. (1) Neointima formation after vascular injury is significantly enhanced in RAMP2+/- mice. (2) Vascular EC-specific RAMP2-deficiency reproduced the phenotype of RAMP2+/- after vascular injury. (3) Both RAMP2+/- and DI-E-RAMP2-/- arteries showed reduced re-endothelialization and enhanced VSMC proliferation (4) Vascular inflammation accompanied by oxidative stress and macrophage infiltration were exacerbated in both RAMP2+/- and DI-E-RAMP2-/- mice. (5) Bone marrow-derived cells contributed to the enhanced neointima formation observed in RAMP2+/- and DI-E-RAMP2-/- mice. (6) The AM-RAMP2 system enhances EPC proliferation and migration. These data clearly show that the endogenous AM-RAMP2 system plays a key role in maintaining vascular homeostasis and inhibiting the progression of atherosclerosis.

Macrophages and inflammatory mediators stimulate VSMC proliferation and neointimal hyperplasia (31). In the present study, we found that inflammatory cell invasion and expression of inflammatory molecules, especially IL-6, MCP-1 and CCR2, were increased in both RAMP2+/- and DI-E-RAMP2 -/- mice after vascular injury. Earlier studies showed that the AM-RAMP system acts to decrease proinflammatory cytokine release (32,33). We reported that the expression of inflammatory adhesion molecules is downregulated by AM *in vivo* (34). Conversely, we found that congenital EC-specific RAMP2-/- mice spontaneously developed vasculitis (18). In the congenital EC-specific RAMP2-/- model, partial detachment of ECs from the basement membrane likely accelerates the attachment, transmigration and accumulation of inflammatory cells within the vascular wall. In addition, the absence of AM-signaling in RAMP2-deficient ECs upregulated expression of inflammatory adhesion molecules and facilitated the attachment of macrophages (18). It is widely recognized that an increase in intracellular cyclic adenosine monophosphate (cAMP) within ECs strengthens their barrier function and reduces endothelial permeability, both *in vitro* and *in vivo* (35,36).

We showed that, in DI-E-RAMP2-/- ECs, downregulation of cAMP production and Rac1 activation reduces cortical actin formation and diminishes endothelial barrier function, which facilitates inflammatory cell adhesion to the ECs (18).

Several lines of evidence suggest that reactive oxygen species (ROS) play a crucial role in neointima formation (37,38). Inflammation augments oxidative stress and vice versa, and the two coordinately promote vascular lesions, acting in a vicious cycle. AM possesses a protective action against cardiovascular damage, possibly through inhibition of ROS production (6). Major sources of ROS are thought to be NADPH oxidase (39). In the present study, we found that the expression of a NADPH subunit, p67phox, was increased in wire-injured arteries from RAMP2+/- and DI-E-RAMP2-/- mice. At the same time, levels of 4HNE, a lipid peroxidation product, were also increased, predominantly in the neointima of the injured arteries. Thus increased ROS production may also contribute the enhanced neointima formation observed in RAMP2+/- and DI-E-RAMP2-/- mice. This suggests that endothelial RAMP2 may be an effective target through which to regulate ROS as well as inflammation.

Re-endothelialization by bone marrow-derived EPCs is an important determinant affecting neointima formation (21,40,41). Bone marrow-derived EPCs are present in peripheral blood and can be recruited to denuded areas and incorporated into nascent endothelium (42,43). EPCs mobilized or transfused systematically are able to home to sites of endothelial denudation, accelerate re-endothelialization of injured arteries, and effectively impair proliferation of VSMCs and neointima formation (44). The role of the AM-RAMP2 system in this process had not been clear. In the present study, therefore, we generated four kinds of BMT mice ($BMT^{WT\rightarrow C57BL/6J}$, $BMT^{RAMP2+/-\rightarrow C57BL/6J}$ or $BMT^{control\rightarrow C57BL/6J}$, $BMT^{DI\text{-}E\text{-}RAMP2\text{-}/-\rightarrow C57BL/6J}$) and evaluated neointima formation following wire-induced injury. We observed that bone marrow-derived cells contributed to the enhanced neointima formation in RAMP2+/- and DI-E-RAMP2-/-, and that vascular re-endothelialization was suppressed and VSMCs were increased in $BMT^{RAMP2+/-\rightarrow C57BL/6J}$ and $BMT^{DI\text{-}E\text{-}RAMP2\text{-}/-\rightarrow C57BL/6J}$ mice. Furthermore, when we cultured primary EPCs from mouse bone marrow and compared the numbers of Dil-Ac-LDL and BS-lection-double positive EPCs, they were smaller in DI-E-RAMP2-/- mice. Thus AM-RAMP2 signaling appears to stimulate the proliferation and mobilization of EPCs.

Based on its structural homology and similar vasodilatory effects, calcitonin gene-related peptide (CGRP) has been classified as an AM family peptide (45) (2). We previously reported that neointima formation is enhanced in CGRP-/- mice following wire-induced vascular injury, but bone marrow-derived cells did not meaningfully contribute to the enhanced neointima formation observed in CGRP-deficient mice (20). AM and CGRP act on the same receptor, CLR, but CGRP acts mainly via CLR with RAMP1 (16). We found that EPCs expressed RAMP2 and CLR; RAMP1 expression was very low (data not shown). After vascular injury, endogenous CGRP may contribute to counteract VSMC proliferation, but have little effect on EPCs.

In summary, RAMP2-deficient mice showed marked neointimal hyperplasia in wire-injured arteries with concomitant suppression re-endothelialization and increased VSMC proliferation. These results clearly demonstrate the AM-RAMP2 system has vasoprotective function following vascular injury, possibly acting in part through stimulation of EPCs proliferation. In our preliminary study, we actually found that RAMP2-overexpression ameliorated vascular lesions (Supplementary Figure 6). We suggest the AM-RAMP2 system could be a novel therapeutic target for treatment of vascular diseases such as atherosclerosis and restenosis after percutaneous coronary intervention.

Sources of funding

This study was supported by Grants-in-Aid for Scientific Research (KAKENHI); Core Research for Evolutionary Science and Technology (CREST) of Japan Science and Technology Agency (JST) and the Japan Agency for Medical Research and Development (AMED); National Cardiovascular Center research grant for cardiovascular diseases; Grants-in aid of The Public Trust Fund For Clinical Cancer Research; Mitsui Life Social Welfare Foundation; Takeda Science Foundation research grant; Opto-Science and Technology research grant; Takeda Medical Research Foundation grant; Elderly Eye Disease Research Foundation grant; Novartis Foundation for Gerontological Research grant; Research grant from the Cosmetology Research Foundation; SENSHIN Medical Research Foundation; Kanzawa Medical Research Foundation; Ono Medical Research Foundation; Nagao Memorial Fund; Nakatomi Foundation; Japan Vascular Disease Research Foundation; YOKOYAMA Foundation for Clinical Pharmacology; and Banyu Life Science Foundation International.

Acknowledgement

VE-cadherin Cre-ERT2 mice ware kindly provided by Dr. Ralf H. Adams, Department of Tissue Morphogenesis, University of Munster

Disclosure statement

None

Figure legends

Figure 1.

Gene expression changes, neointimal hyperplasia, vascular re-endothelialization and VSMC proliferation after wire-induced vascular injury in RAMP2+/- and WT mice. Femoral arteries were excised on day 14 or 28 after injury. **A,** Quantitative real-time PCR analysis of relative expression of AM and RAMP genes in WT mice with (Injury) or without (Sham) wire-induced vascular injury. Mean of the sham group was assigned a value of 1. Bars indicate means ± SE (n=5 for each); *p<0.05 vs. sham-operated WT mice. **B,** Relative expression of AM and RAMP genes in WT and RAMP2+/- mice after sham operation (left) or wire injury (right). Mean of the WT group was assigned a value of 1. Bars depict means ± SE (n=6-10 for each); *p<0.05, **p<0.01 vs. WT. **C,** Representative EVG-stained sections used to evaluate neointima formation. Femoral arteries were collected 14 and 28 days after wire injury. The arrows indicate the internal elastic lamina. (n=6-10 in each group). Bar = 100 μm. **D, E,** Bar graphs showing the medial area, neointimal area (**D**) and neointima/media ratio (**E**). Bars depict means ± SE (n=6-10 for each); *p<0.05, **p<0.01 vs. WT. **F, G** Evaluation of re-endothelialization and VSMC proliferation. **F**, Representative images showing immunohistochemical staining for ECs (CD31; red) and VSMCs (α-SMA; green). The percentages of the lumen perimeter that was CD31 positive in femoral cross-sections were evaluated. Bars = 100 μm. **G**, Bar graphs showing the percentages of re-endothelialization in the injured area (upper panel) and α-SMA-positive area (lower panel). Bars depict means ± SE (n=6-10 for each); **p<0.01 vs. WT.

Figure 2. Inflammatory cell invasion and inflammatory cytokine expression were higher in RAMP2+/- than WT mice after wire injury. **A,** Representative femoral arterial sections showing immunohistochemical staining for macrophages (F4/80) in sham-operated and injured arteries collected from WT and RAMP2+/- mice on day 28 after injury. Bars = 100 μm. **B,** Bar graphs showing F4/80-positive macrophage numbers in the adventitial and neointimal areas within each section. Bars depict means ± SE (n=6-10 for each); **p<0.01 vs. WT. **C,** Quantitative real-time PCR analysis of the indicated inflammatory molecules and macrophage markers in sham-operated and injured arteries collected on days 14 and 28 after wire injury. Bars depict means ± SE (n=3-5 for each

in 2 independent experiments); *P<0.05 vs. WT. Mean of the WT group was assigned a value of 1.

Figure 3. Increased oxidative stress within neointimal lesions in RAMP2+/- mice. **A,** Representative photomicrographs (n=3-5 for each group) showing immunohistochemical staining for p67phox. Bars = 100 μm. **B,** Quantitative real-time PCR analysis of the indicated oxidative stress-related genes in sham-operated (upper panel) and injured arteries collected on day 28 after wire injury (lower panel). Mean of the WT group was assigned a value of 1. Bars depict means ± SE (n=6-10 for each); *P<0.05 vs. WT. **C,** Representative photomicrographs (n=3-5 for each group) showing immunohistochemical staining for 4HNE. Bars = 100 μm.

Figure 4. Gene expression changes, neointimal hyperplasia, vascular re-endothelialization and VSMC proliferation after wire-induced vascular injury of drug-inducible endothelial cell-specific RAMP2-/- mice (DI-E-RAMP2-/-) and their control mice. Femoral arteries were excised on day 14 or 28 after vascular injury. **A,** Quantitative real-time PCR analysis of relative expression of AM and RAMP genes in control mice (Cont) with (Injury Day 28) and without (Sham) vascular injury. Mean of the sham group was assigned a value of 1. Bars indicate means ± SE (n=5 for each); *p<0.05 vs. sham-operated control mice. **B,** Relative expression of AM and RAMP genes in control and DI-E-RAMP2-/- mice after sham operation (left) and vascular injury (right). Mean of the control group was assigned a value of 1. Bars depict means ± SE (n=6-10 for each); *p<0.05, **p<0.01 vs. WT. **C,** Representative EVG-stained sections used to evaluate neointima formation. Femoral arteries were collected on days 14 and 28 after vascular injury. The arrows indicate the internal elastic lamina. (n=6-10 in each group). Bars = 100 μm. **D, E,** Bar graphs showing the medial areas, neointimal areas (**D**) and neointima/media ratios (**E**). Bars depict means ± SE (n=6-10 for each); *p<0.05, **p<0.01 vs. WT. **F, G,** Evaluation of re-endothelialization and VSMC proliferation. **F**, Representative images of immunohistochemical staining for ECs (CD31; red) and VSMCs (α-SMA; green). Bars = 100 μm. **G**, Bar graphs showing the percent of re-endothelialization in the injured area (upper panel) and comparison of α-

SMA-positive areas (lower panel). Bars depict means ± SE (n=6-10 for each); **p<0.01 vs. control.

Figure 5. Inflammatory cell invasion and inflammatory cytokine expression in wire-injured arteries was reduced in DI-E-RAMP2 -/- mice. **A,** Representative femoral arterial sections showing immunohistochemical staining for macrophages (F4/80) in sham-operated and injured arteries from control and DI-E-RAMP2-/- mice on day 28 after wire injury. Bars = 100 μm. **B,** Bar graphs showing F4/80-positive macrophage numbers in adventitial and neointimal areas within each section. Bars depict means ± SE (n=6-10 for each); **p<0.01 vs. control. **C,** Quantitative real-time PCR analysis of the indicated inflammatory cytokines and macrophage markers in sham-operated and injured arteries on days 14 and 28 after wire injury. Bars depict means ± SE (n=3-5 for each from 2 independent experiments); *P<0.05 vs. control. Mean of the WT group was assigned a value of 1.

Figure 6. Increased oxidative stress within neointimal lesions in DI-E-RAMP2 -/- mice. **A,** Representative photomicrographs (n=3-5 for each group) showing immunohistochemical staining for p67phox. Bars = 100 μm. **B,** Quantitative real-time PCR analysis of the indicated oxidative stress-related genes in sham-operated (upper panel) and injured arteries on day 28 after wire injury (lower panel). Mean of the control group was assigned a value of 1. Bars depict means ± SE (n=6-10 for each); *P<0.05 vs. control. **C,** Representative photomicrographs (n=3-5 for each group) showing immunohistochemical staining for 4HNE. Bars = 100 μm.

Figure 7. Bone marrow-derived cells contribute to the enhanced neointimal formation detected in RAMP2+/- mice. Bone marrow transplantation (BMT) was performed from WT to C57BL/6J mice ($BMT^{WT \rightarrow C57BL/6J}$ (n=16)) or from RAMP2+/- to C57BL/6J mice ($BMT^{RAMP2+/- \rightarrow C57BL/6J}$ (n=16)). Femoral arteries were subjected to wire-induced injury 8 weeks after BMT and excised 28 days after injury. Neointimal hyperplasia (**A, B**), vascular re-endothelialization and VSMC proliferation (**C, D**) were evaluated. **A**, Representative photomicrographs of EVG-stained arteries following wire injury. The arrows indicate the internal elastic lamina. Bars = 100 μm. **B**, Bar graphs showing the

neointimal and medial areas (left) and intima/media ratios (right). Bars depict means ± SE. **C**, Representative images of immunohistochemical staining form ECs (CD31; red) and VSMCs (α-SMA; green). Bars = 100 μm. **D**, Bar graphs showing the percent of re-endothelialization in the injured area (left) and comparison of α-SMA-positive areas (right). Bars depict means ± SE (n=6-10 for each); *p<0.05, **p<0.01 vs. $BMT^{WT \rightarrow C57BL/6J}$.

Figure 8. Bone marrow-derived cells contribute to the enhanced neointimal formation in DI-E-RAMP2-/- mice. Bone marrow transplantation (BMT) was performed from control to C57BL/6J mice ($BMT^{Cont \rightarrow C57BL/6J}$ (n=16)) or from DI-E-RAMP2-/- to C57BL/6J mice ($BMT^{DI\text{-}E\text{-}RAMP2\text{-}/- \rightarrow C57BL/6J}$ (n=16)). Femoral arteries were excised 28 days after injury. Neointimal hyperplasia (**A, B**), vascular re-endothelialization and VSMC proliferation (**C, D**) were evaluated. **A,** Representative photomicrographs of EVG-stained arteries following wire injury in bone marrow-transplanted mice. The arrows indicate the internal elastic lamina. Bars = 100 μm. **B**, Bar graphs showing the neointimal and medial areas (left) and intima/media ratios (right). Bars depict means ± SE. **C**, Representative images of immunohistochemical staining for ECs (CD31; red) and VSMCs (α-SMA; green). Bars = 100 μm. **D**, Bar graphs showing the percent of re-endothelialization in the injured area (left) and comparison of α-SMA-positive areas (right). Bars depict means ± SE (n=6-10 for each); **p<0.01vs. $BMT^{Cont \rightarrow C57BL/6J}$.

Figure 9. AM-RAMP2 signaling potentiated endothelial progenitor cells (EPCs) proliferation and migration *in vitro.* **A,** Evaluation of EPCs cultured from bone marrow collected from control and DI-E-RAMP2-/- mice. In the culture dish, Dil-Ac-LDL uptake and staining for BS-1 lectin were analyzed. (x200 magnification). **B**, Bar graphs showing the comparison of the Dil-Ac-LDL and BS-lection double-positive cell number per field. Bars depict means ± SE (n=12 for each). **p<0.01. In DI-E-RAMP2-/-, the number of EPCs was reduced compared with control. **C,** RT-PCR analysis of AM, RAMP2 and CLR in human EPCs. **D,** WST cell proliferation assays of human EPCs. Bars depict means ± SE (n=10 for each). *p<0.05. AM administration significantly enhanced proliferation of human EPCs. **E,** Representative photos of tube formation assay on Matrigel matrix (x40 magnification). **F,** Measured tubule lengths presented as

the ratio of control. Bars depict means ± SE (n=16 for each). **p<0.01. AM (10^{-7}M) administration significantly enhanced the tube formation.

Supplementary Figure legends

Supplementary Figure 1.

Time course of the change of RAMP2 gene expression after the induction of the gene deletion. After 5 days of tamoxifen-treatment, endothelial cells were isolated from 8 week-old DI-E-RAMP2-/- mice. Mean of the control group was assigned a value of 1. Vertical bars indicate mean ± SE (n=3 for each).

Supplementary Figure 2.

Measurement of the serum AM levels. **A,** Comparison of serum AM levels in control and DI-E-RAMP2-/- mice. Bars depict mean ± SE (n=8 in each group). **B,** Comparison of serum AM levels among BMT recipient mice. Bone marrow transplantation (BMT) was performed from control to C57BL/6J mice ($BMT^{Cont\rightarrow C57BL/6J}$) or from DI-E-RAMP2-/- to C57BL/6J mice ($BMT^{DI\text{-}E\text{-}RAMP2\text{-}/\text{-}\rightarrow C57BL/6J}$). Bars depict mean ± SE (n=5 in each group).

Supplementary Figure 3.

Comparison of the effect of tamoxifien between control corn oil in VE-cadherin-Cre transgenic mice (without the flox region). **A,** Representative EVG-stained sections used to evaluate neointima formation. Femoral arteries were collected 28 days after wire injury. The arrows indicate the internal elastic lamina. Bar = 100 μm. **B, C,** Bar graphs showing the medial area, neointimal area (**B**) and neointima/media ratio (**C**). Bars depict mean ± SE (n=4 in each group). Tamoxifen-treatment itself did not have an effect on the media, neointima (**A, B**) and neointima/media ratio (**C**).

Supplementary Figure 4.

Comparison of systolic blood pressure between control and DI-E-RAMP2-/ male mice using tail cuff method. Bars depict mean ± SE (n=4 in each group).

Supplementary Figure 5.

Comparison of the RAMP2 gene-expression in the cells isolated from bone marrow of DI-E-RAMP2 treated with 5 days of tamoxifen or control corn oil and maintained under the EPC culture condition. Bars indicate mean ± SE (n=10 for each). *$p<0.05$ vs. control. In DI-E-RAMP2-/-, the RAMP2 gene expression was significantly reduced compared with control.

Supplementary Figure 6.

Comparison of the neointima formation by the wire-injury between control and endothelial-cell specific RAMP2-overexpressing transgenic mice (RAMP2 Tg). **A,** Representative EVG-stained sections used to evaluate neointima formation. Femoral arteries were collected 28 days after wire injury. The arrows indicate the internal elastic lamina. Bar = 100 μm. **B, C,** Bar graphs showing the medial area, neointimal area (**B**) and neointima/media ratio (**C**). Bars depict mean ± SE (n=4 in each group).

Primers and probes used for quantitative real-time RT-PCR (mouse)

AM Forward	**CTACCGCCAGAGCATGAACC**	**MCP-1 Forward**	**GCAGTTAACGCCCCACTCA**
AM Reverse	**GAAATGTGCAGGTCCCGAA**	**MCP-1Reverse**	**CCTACTCATTGGGATCATCTTGCT**
AM Probe	**CCCGCAGCAATGGATGCCG**	**IL-1β Forward**	**TCTCACAGCAGCACATCAAC**
CLR Forward	**AGGCGTTTACCTGCACACACT**	**IL-1β Reverse**	**TCGTTGCTTGGTTCTCCTTG**
CLR Reverse	**CAGGAAGCAGAGGAAACCCC**	**IL-6 Forward**	**TGAATTGGATGGTCTTGGTCC**
CLR Probe	**ATCGTGGTGGCTGTGTTTGCGGAG**	**IL-6 Reverse**	**TGAATTGGATGGTCTTGGTCC**
RAMP1 Forward	**CGCACACGATTGGCTGTTT**	**TNF-α Forward**	**ACGGCATGGATCAAAGAC**
RAMP1 Reverse	**TGGTGGACAGCGATGAAGAA**	**TNF-α Reverse**	**AGATAGCAAATCGGCTGACG**
RAMP2 Forward	**GCAGCCCACCTTCTCTGATC**	**TGF-β1 Forward**	**CCCGAAGCGGACTACTATGC**
RAMP2 Reverse	**AACGGGATGAGGCAGATGG**	**TGF-β1 Reverse**	**TAGATGGCGTTGTTGCGGT**
RAMP2 Probe	**CCCAGAGGATGTGCTCCTGGCCAT**	**eNOS Forward**	**ACGGCATGGATCAAAGAC**
RAMP3 Forward	**TGCAACGAGACAGGGATGC**	**eNOS Reverse**	**AGATAGCAAATCGGCTGACG**
RAMP3 Reverse	**GCATCATGTCAGCGAAGGC**	**p67phox Forward**	**CAGACCCAAAACCCCAGAAA**
RAMP3 Probe	**AGAGGCTGCCTCGCTGTGGGAA**	**p67phox Reverse**	**AAAGCCAAACAATACGCGGT**
F4/80Forward	**GATGAATTCCCGTGTTGTTGGT**	**p47phox Forward**	**ATCCTATCTGGACCCCTTGA**
F4/80 Reverse	**ACATCAGTGTTCCAGGAGACACA**	**p47phox Reverse**	**CACCTGCGTAGTTGGGATCC**
CCR2 Forward	**GCTCAACTTGGCCATCTCTGA**	**P22phox Forward**	**GGCCATTGCCAGTGTGATCT**
CCR2 Reverse	**AGACCCACTCATTTGCAGCAT**	**P22phox Reverse**	**GCTCAATGGGAGTCCACTGC**
CD68 Forward	**TGGCGGTGGAATACAATGTG**		
CD68 Reverse	**GAGATGAATTCTGCGCCATGA**		

Table. 1.

Primers used for RT-PCR (Human)

AM Forward	**TAAGTGGGCTCTGAGTCGTG**
AM Reverse	**CGTGTGCTTGTGGCTTAGAA**
CLR Forward	**CAAGACCCCATTCAACAAGC**
CLR Reverse	**AATGCCTTCACAGAGCATCC**
RAMP2 Forward	**GAACTATGAGACAGCTGTCC**
RAMP2 Reverse	**CCTGGGCCTCACTGTCTTTA**

Table. 2.

References

1. Ross R. Atherosclerosis--an inflammatory disease. N Engl J Med 1999; 340:115-126
2. Kitamura K, Kangawa K, Kawamoto M, Ichiki Y, Nakamura S, Matsuo H, Eto T. Adrenomedullin: a novel hypotensive peptide isolated from human pheochromocytoma. Biochem Biophys Res Commun 1993; 192:553-560
3. Abe M, Sata M, Nishimatsu H, Nagata D, Suzuki E, Terauchi Y, Kadowaki T, Minamino N, Kangawa K, Matsuo H, Hirata Y, Nagai R. Adrenomedullin augments collateral development in response to acute ischemia. Biochemical and biophysical research communications 2003; 306:10-15
4. Kato K, Yin H, Agata J, Yoshida H, Chao L, Chao J. Adrenomedullin gene delivery attenuates myocardial infarction and apoptosis after ischemia and reperfusion. American journal of physiology Heart and circulatory physiology 2003; 285:H1506-1514
5. Isumi Y, Kubo A, Katafuchi T, Kangawa K, Minamino N. Adrenomedullin suppresses interleukin-1beta-induced tumor necrosis factor-alpha production in Swiss 3T3 cells. FEBS Lett 1999; 463:110-114
6. Shimosawa T, Shibagaki Y, Ishibashi K, Kitamura K, Kangawa K, Kato S, Ando K, Fujita T. Adrenomedullin, an endogenous peptide, counteracts cardiovascular damage. Circulation 2002; 105:106-111
7. Nishikimi T, Matsuoka H. Cardiac adrenomedullin: its role in cardiac hypertrophy and heart failure. Curr Med Chem Cardiovasc Hematol Agents 2005; 3:231-242
8. Petrie MC, Hillier C, Morton JJ, McMurray JJ. Adrenomedullin selectively inhibits angiotensin II-induced aldosterone secretion in humans. J Hypertens 2000; 18:61-64
9. Samson WK, Murphy T, Schell DA. A novel vasoactive peptide, adrenomedullin, inhibits pituitary adrenocorticotropin release. Endocrinology 1995; 136:2349-2352
10. Shimosawa T, Ogihara T, Matsui H, Asano T, Ando K, Fujita T. Deficiency of adrenomedullin induces insulin resistance by increasing oxidative stress. Hypertension 2003; 41:1080-1085
11. Ishimitsu T, Nishikimi T, Saito Y, Kitamura K, Eto T, Kangawa K, Matsuo H, Omae T, Matsuoka H. Plasma levels of adrenomedullin, a newly identified hypotensive peptide, in patients with hypertension and renal failure. J Clin Invest 1994; 94:2158-2161
12. Nishikimi T, Saito Y, Kitamura K, Ishimitsu T, Eto T, Kangawa K, Matsuo H, Omae T, Matsuoka H. Increased plasma levels of adrenomedullin in patients with heart failure. J Am Coll Cardiol 1995; 26:1424-1431
13. Hojo Y, Ikeda U, Katsuki TA, Shimada K. Decreased adrenomedullin production in the coronary circulation of patients with coronary artery disease. Heart 2000; 84:88
14. Hojo Y, Ikeda U, Mizuno O, Katsuki TA, Shimada K. Adrenomedullin expression in coronary circulation after stent implantation as a prognostic factor for restenosis. Int J Cardiovasc Intervent 2003; 5:190-194
15. Imai Y, Shindo T, Maemura K, Sata M, Saito Y, Kurihara Y, Akishita M, Osuga J, Ishibashi S, Tobe K, Morita H, Oh-hashi Y, Suzuki T, Maekawa H, Kangawa

K, Minamino N, Yazaki Y, Nagai R, Kurihara H. Resistance to neointimal hyperplasia and fatty streak formation in mice with adrenomedullin overexpression. Arterioscler Thromb Vasc Biol 2002; 22:1310-1315
16. McLatchie LM, Fraser NJ, Main MJ, Wise A, Brown J, Thompson N, Solari R, Lee MG, Foord SM. RAMPs regulate the transport and ligand specificity of the calcitonin-receptor-like receptor. Nature 1998; 393:333-339
17. Ichikawa-Shindo Y, Sakurai T, Kamiyoshi A, Kawate H, Iinuma N, Yoshizawa T, Koyama T, Fukuchi J, Iimuro S, Moriyama N, Kawakami H, Murata T, Kangawa K, Nagai R, Shindo T. The GPCR modulator protein RAMP2 is essential for angiogenesis and vascular integrity. J Clin Invest 2008; 118:29-39
18. Koyama T, Ochoa-Callejero L, Sakurai T, Kamiyoshi A, Ichikawa-Shindo Y, Iinuma N, Arai T, Yoshizawa T, Iesato Y, Lei Y, Uetake R, Okimura A, Yamauchi A, Tanaka M, Igarashi K, Toriyama Y, Kawate H, Adams RH, Kawakami H, Mochizuki N, Martinez A, Shindo T. Vascular endothelial adrenomedullin-RAMP2 system is essential for vascular integrity and organ homeostasis. Circulation 2013; 127:842-853
19. Sata M, Maejima Y, Adachi F, Fukino K, Saiura A, Sugiura S, Aoyagi T, Imai Y, Kurihara H, Kimura K, Omata M, Makuuchi M, Hirata Y, Nagai R. A mouse model of vascular injury that induces rapid onset of medial cell apoptosis followed by reproducible neointimal hyperplasia. J Mol Cell Cardiol 2000; 32:2097-2104
20. Yang L, Sakurai T, Kamiyoshi A, Ichikawa-Shindo Y, Kawate H, Yoshizawa T, Koyama T, Iesato Y, Uetake R, Yamauchi A, Tanaka M, Toriyama Y, Igarashi K, Shindo T. Endogenous CGRP protects against neointimal hyperplasia following wire-induced vascular injury. J Mol Cell Cardiol 2013; 59:55-66
21. Yoshioka T, Takahashi M, Shiba Y, Suzuki C, Morimoto H, Izawa A, Ise H, Ikeda U. Granulocyte colony-stimulating factor (G-CSF) accelerates reendothelialization and reduces neointimal formation after vascular injury in mice. Cardiovasc Res 2006; 70:61-69
22. Ii M, Takenaka H, Asai J, Ibusuki K, Mizukami Y, Maruyama K, Yoon YS, Wecker A, Luedemann C, Eaton E, Silver M, Thorne T, Losordo DW. Endothelial progenitor thrombospondin-1 mediates diabetes-induced delay in reendothelialization following arterial injury. Circ Res 2006; 98:697-704
23. Tanaka K, Sata M, Hirata Y, Nagai R. Diverse contribution of bone marrow cells to neointimal hyperplasia after mechanical vascular injuries. Circ Res 2003; 93:783-790
24. Yajima N, Takahashi M, Morimoto H, Shiba Y, Takahashi Y, Masumoto J, Ise H, Sagara J, Nakayama J, Taniguchi S, Ikeda U. Critical role of bone marrow apoptosis-associated speck-like protein, an inflammasome adaptor molecule, in neointimal formation after vascular injury in mice. Circulation 2008; 117:3079-3087
25. Sata M, Saiura A, Kunisato A, Tojo A, Okada S, Tokuhisa T, Hirai H, Makuuchi M, Hirata Y, Nagai R. Hematopoietic stem cells differentiate into vascular cells that participate in the pathogenesis of atherosclerosis. Nature medicine 2002; 8:403-409
26. Sugo S, Minamino N, Kangawa K, Miyamoto K, Kitamura K, Sakata J, Eto T, Matsuo H. Endothelial cells actively synthesize and secrete adrenomedullin.

Biochem Biophys Res Commun 1994; 201:1160-1166
27. Sugo S, Minamino N, Shoji H, Kangawa K, Kitamura K, Eto T, Matsuo H. Production and secretion of adrenomedullin from vascular smooth muscle cells: augmented production by tumor necrosis factor-alpha. Biochem Biophys Res Commun 1994; 203:719-726
28. Shindo T, Kurihara Y, Nishimatsu H, Moriyama N, Kakoki M, Wang Y, Imai Y, Ebihara A, Kuwaki T, Ju KH, Minamino N, Kangawa K, Ishikawa T, Fukuda M, Akimoto Y, Kawakami H, Imai T, Morita H, Yazaki Y, Nagai R, Hirata Y, Kurihara H. Vascular abnormalities and elevated blood pressure in mice lacking adrenomedullin gene. Circulation 2001; 104:1964-1971
29. Kato H, Shichiri M, Marumo F, Hirata Y. Adrenomedullin as an autocrine/paracrine apoptosis survival factor for rat endothelial cells. Endocrinology 1997; 138:2615-2620
30. Kano H, Kohno M, Yasunari K, Yokokawa K, Horio T, Ikeda M, Minami M, Hanehira T, Takeda T, Yoshikawa J. Adrenomedullin as a novel antiproliferative factor of vascular smooth muscle cells. J Hypertens 1996; 14:209-213
31. Hamaya R, Ogawa M, Suzuki J, Kobayashi N, Hirata Y, Nagai R, Komuro I, Isobe M. A selective peroxisome proliferator-activated receptor-beta/delta agonist attenuates neointimal hyperplasia after wire-mediated arterial injury. Expert Opin Investig Drugs 2013; 22:1095-1106
32. Miksa M, Wu R, Cui X, Dong W, Das P, Simms HH, Ravikumar TS, Wang P. Vasoactive hormone adrenomedullin and its binding protein: anti-inflammatory effects by up-regulating peroxisome proliferator-activated receptor-gamma. J Immunol 2007; 179:6263-6272
33. Hippenstiel S, Witzenrath M, Schmeck B, Hocke A, Krisp M, Krull M, Seybold J, Seeger W, Rascher W, Schutte H, Suttorp N. Adrenomedullin reduces endothelial hyperpermeability. Circ Res 2002; 91:618-625
34. Iinuma N, Sakurai T, Kamiyoshi A, Ichikawa-Shindo Y, Arai T, Yoshizawa T, Koyama T, Uetake R, Kawate H, Muto S, Tagawa Y, Miyagawa S, Shindo T. Adrenomedullin in sinusoidal endothelial cells play protective roles against cold injury of liver. Peptides 2010; 31:865-871
35. Temmesfeld-Wollbruck B, Hocke AC, Suttorp N, Hippenstiel S. Adrenomedullin and endothelial barrier function. Thromb Haemost 2007; 98:944-951
36. Prasain N, Stevens T. The actin cytoskeleton in endothelial cell phenotypes. Microvasc Res 2009; 77:53-63
37. Shi Y, Niculescu R, Wang D, Patel S, Davenpeck KL, Zalewski A. Increased NAD(P)H oxidase and reactive oxygen species in coronary arteries after balloon injury. Arterioscler Thromb Vasc Biol 2001; 21:739-745
38. Patterson C, Ruef J, Madamanchi NR, Barry-Lane P, Hu Z, Horaist C, Ballinger CA, Brasier AR, Bode C, Runge MS. Stimulation of a vascular smooth muscle cell NAD(P)H oxidase by thrombin. Evidence that p47(phox) may participate in forming this oxidase in vitro and in vivo. J Biol Chem 1999; 274:19814-19822
39. Schramm A, Matusik P, Osmenda G, Guzik TJ. Targeting NADPH oxidases in vascular pharmacology. Vascular pharmacology 2012; 56:216-231
40. Kong D, Melo LG, Gnecchi M, Zhang L, Mostoslavsky G, Liew CC, Pratt RE, Dzau VJ. Cytokine-induced mobilization of circulating endothelial progenitor cells enhances repair of injured arteries. Circulation 2004; 110:2039-2046

41. Gulati R, Jevremovic D, Peterson TE, Witt TA, Kleppe LS, Mueske CS, Lerman A, Vile RG, Simari RD. Autologous culture-modified mononuclear cells confer vascular protection after arterial injury. Circulation 2003; 108:1520-1526
42. Walter DH, Rittig K, Bahlmann FH, Kirchmair R, Silver M, Murayama T, Nishimura H, Losordo DW, Asahara T, Isner JM. Statin therapy accelerates reendothelialization: a novel effect involving mobilization and incorporation of bone marrow-derived endothelial progenitor cells. Circulation 2002; 105:3017-3024
43. Sorrentino SA, Bahlmann FH, Besler C, Muller M, Schulz S, Kirchhoff N, Doerries C, Horvath T, Limbourg A, Limbourg F, Fliser D, Haller H, Drexler H, Landmesser U. Oxidant stress impairs in vivo reendothelialization capacity of endothelial progenitor cells from patients with type 2 diabetes mellitus: restoration by the peroxisome proliferator-activated receptor-gamma agonist rosiglitazone. Circulation 2007; 116:163-173
44. Iwakura A, Luedemann C, Shastry S, Hanley A, Kearney M, Aikawa R, Isner JM, Asahara T, Losordo DW. Estrogen-mediated, endothelial nitric oxide synthase-dependent mobilization of bone marrow-derived endothelial progenitor cells contributes to reendothelialization after arterial injury. Circulation 2003; 108:3115-3121
45. Rosenfeld MG, Mermod JJ, Amara SG, Swanson LW, Sawchenko PE, Rivier J, Vale WW, Evans RM. Production of a novel neuropeptide encoded by the calcitonin gene via tissue-specific RNA processing. Nature 1983; 304:129-135

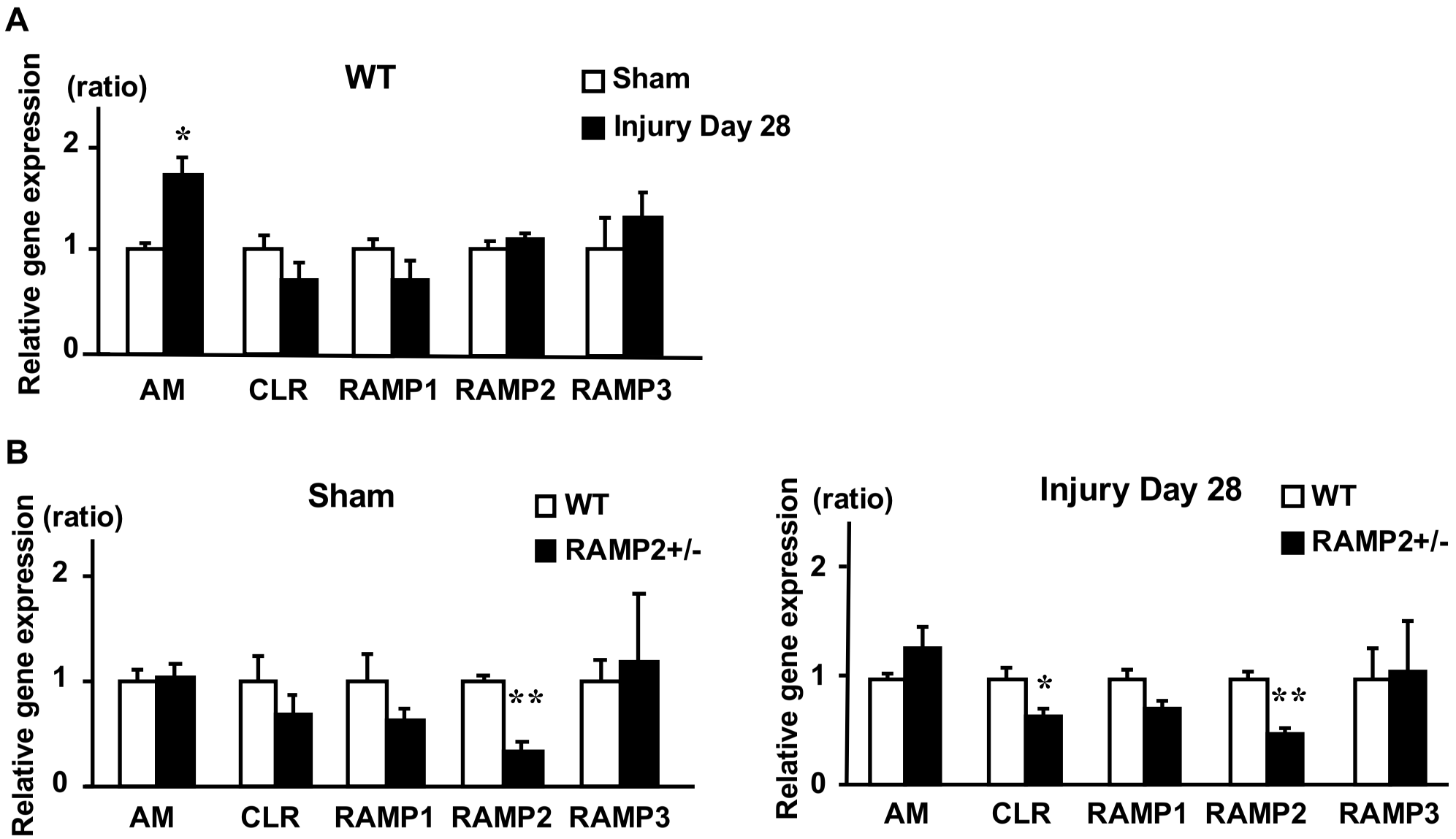
A
WT
Sham
Injury Day 28
(ratio)
Relative gene expression
2
1
0
*
AM
CLR
RAMP1
RAMP2
RAMP3
B
Sham
WT
RAMP2+/-
(ratio)
Relative gene expression
2
1
0
**
AM
CLR
RAMP1
RAMP2
RAMP3
Injury Day 28
WT
RAMP2+/-
(ratio)
Relative gene expression
2
1
0
*
**
AM
CLR
RAMP1
RAMP2
RAMP3

Fig. 1

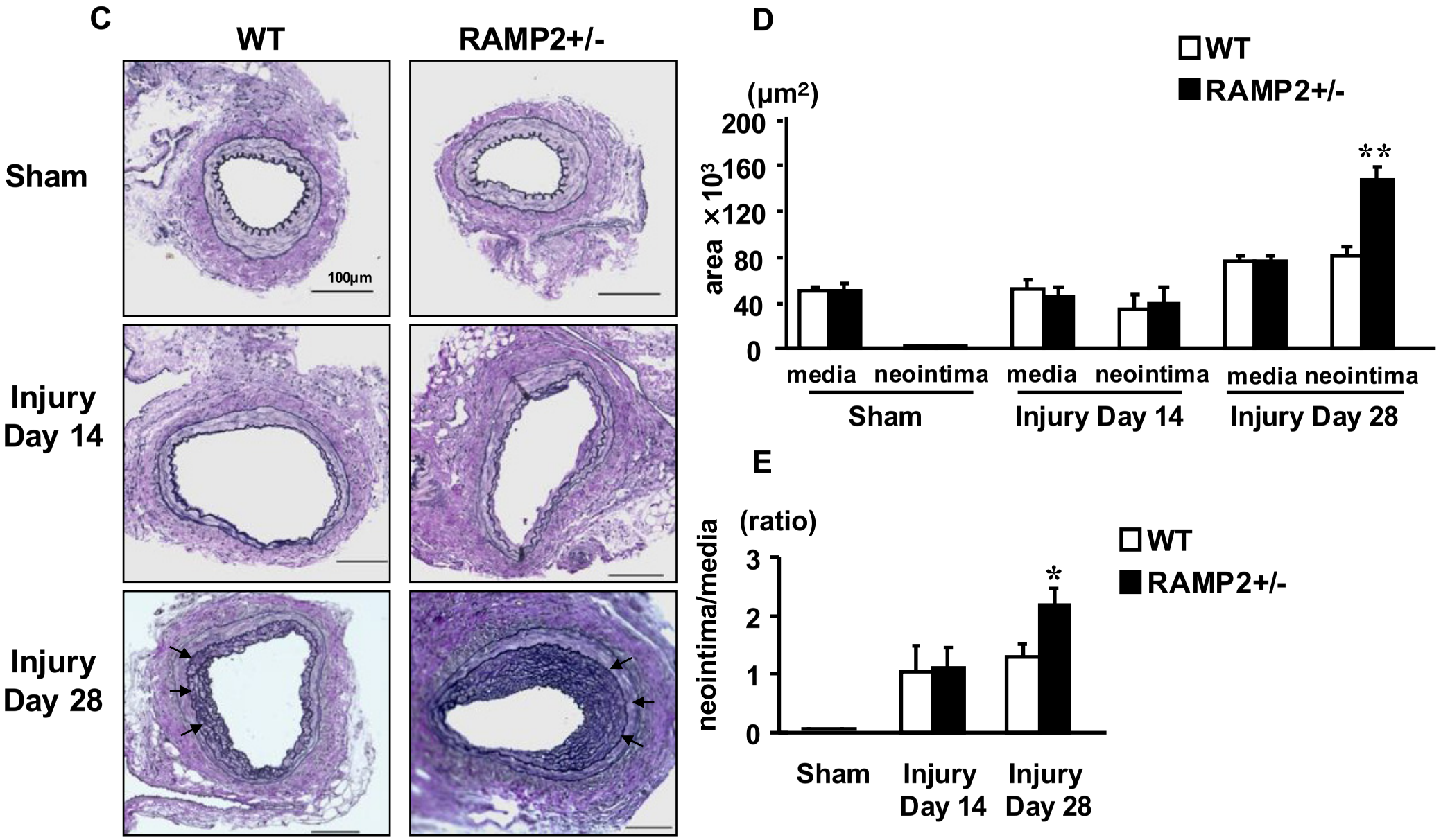
C
WT
RAMP2+/-
Sham
Injury Day 14
Injury Day 28
100μm
D
WT
RAMP2+/-
(μm²)
area ×10³
200
160
120
80
40
0
**
media
neointima
media
neointima
media
neointima
Sham
Injury Day 14
Injury Day 28
E
(ratio)
neointima/media
3
2
1
0
*
WT
RAMP2+/-
Sham
Injury Day 14
Injury Day 28

Fig. 1

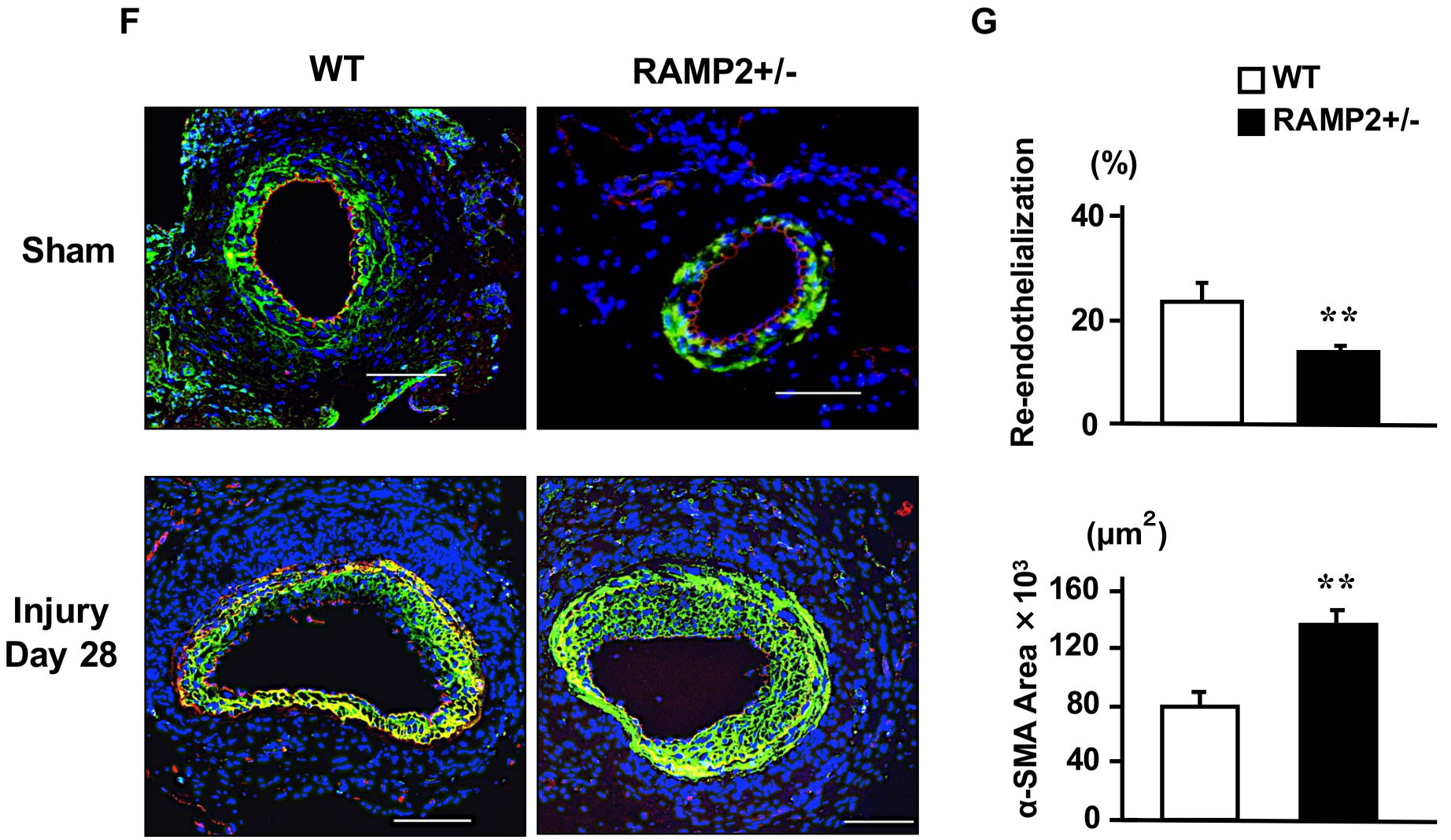
F
WT
RAMP2+/-
Sham
Injury
Day 28
G
WT
RAMP2+/-
Re-endothelialization
(%)
40
20
0
**
α-SMA Area × 10³
(μm²)
160
120
80
40
0
**

Fig. 1

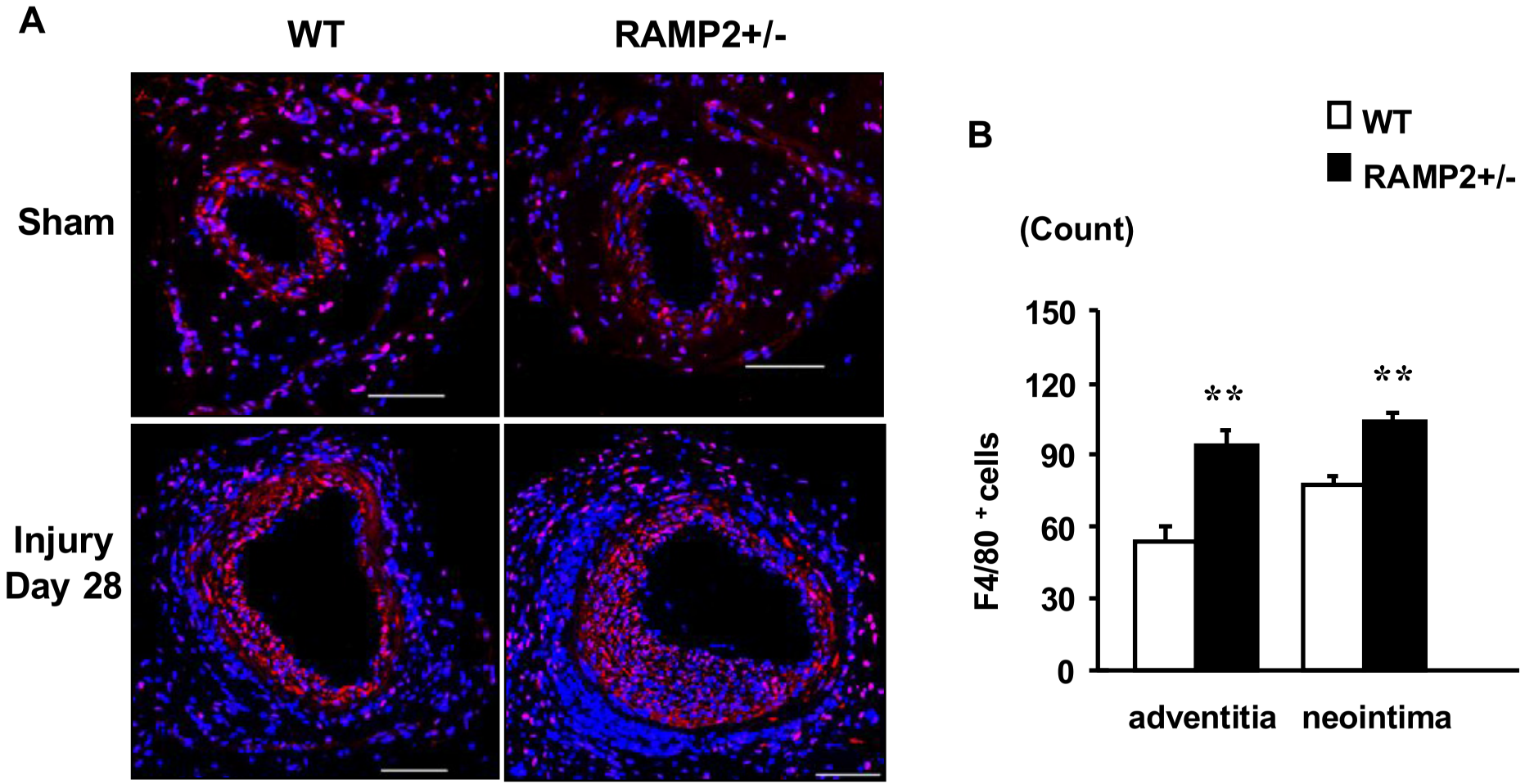
A
WT
RAMP2+/-
Sham
Injury
Day 28
B
WT
RAMP2+/-
(Count)
F4/80 + cells
150
120
90
60
30
0
**
**
adventitia
neointima

Fig. 2

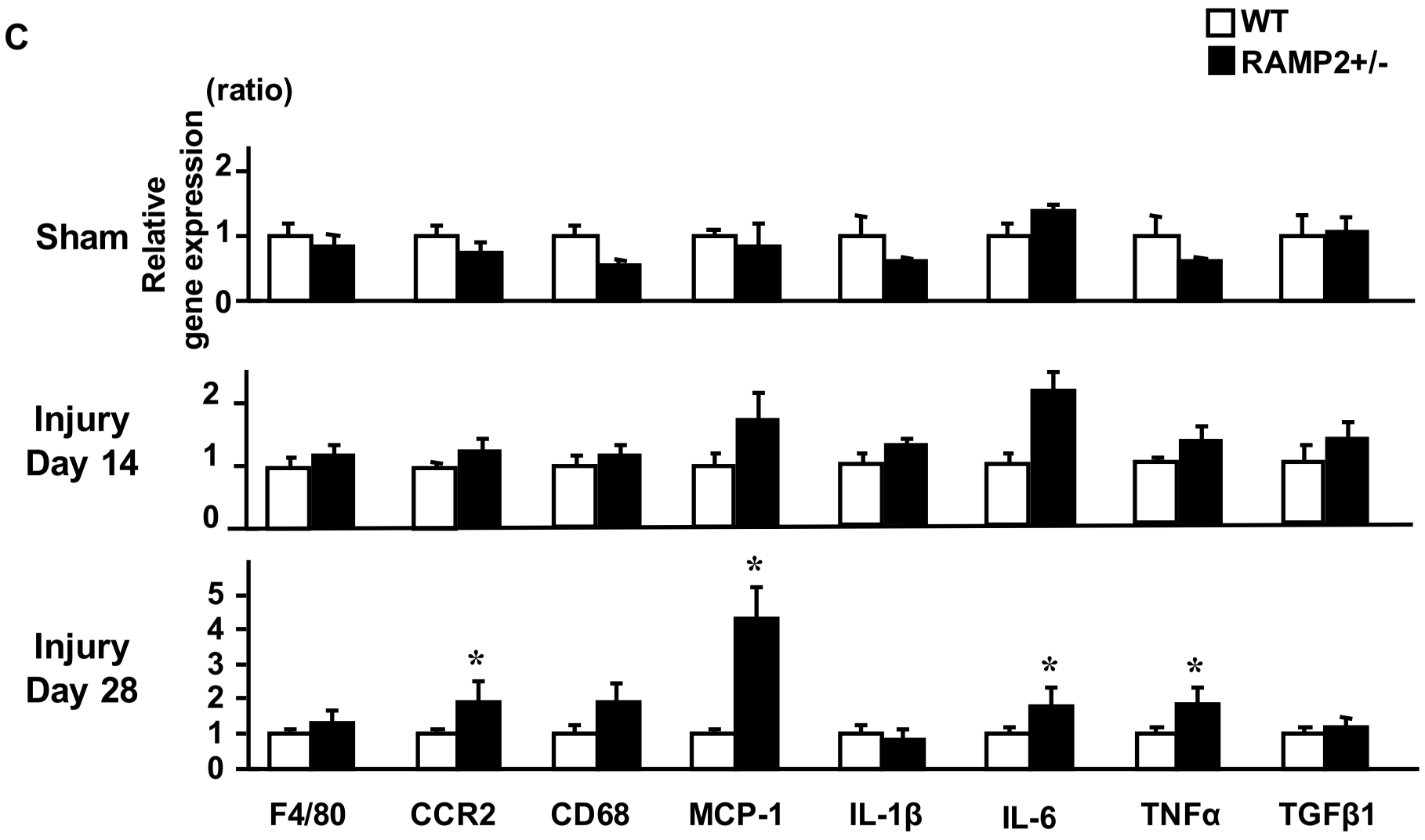
C
WT
RAMP2+/-
Relative gene expression (ratio)
Sham
Injury Day 14
Injury Day 28
0
1
2
0
1
2
0
1
2
3
4
5
*
*
*
*
F4/80
CCR2
CD68
MCP-1
IL-1β
IL-6
TNFα
TGFβ1

Fig. 2

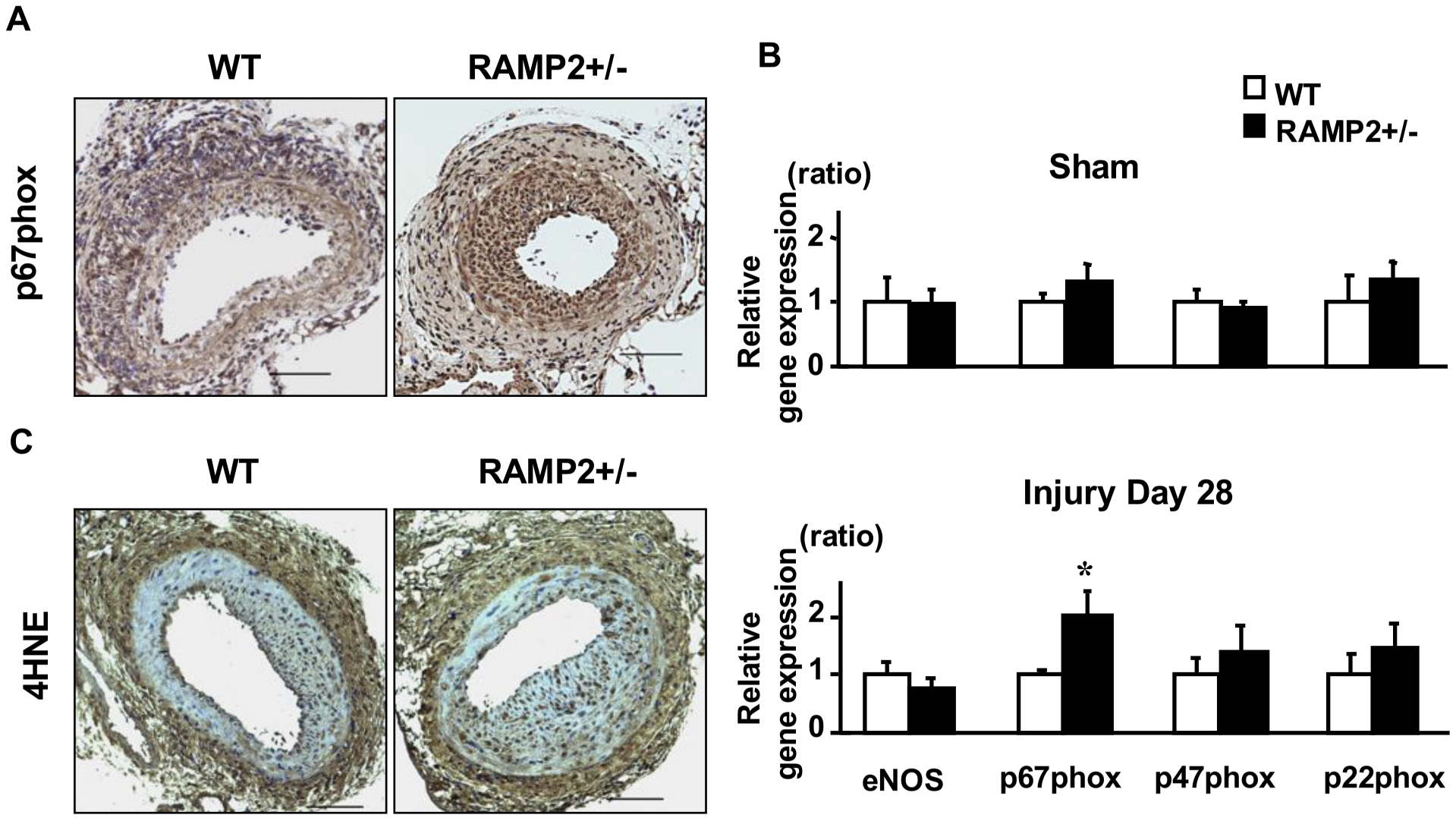
A
WT
RAMP2+/-
p67phox
B
WT
RAMP2+/-
Sham
(ratio)
Relative gene expression
2
1
0
C
WT
RAMP2+/-
4HNE
Injury Day 28
(ratio)
Relative gene expression
*
2
1
0
eNOS
p67phox
p47phox
p22phox

Fig. 3

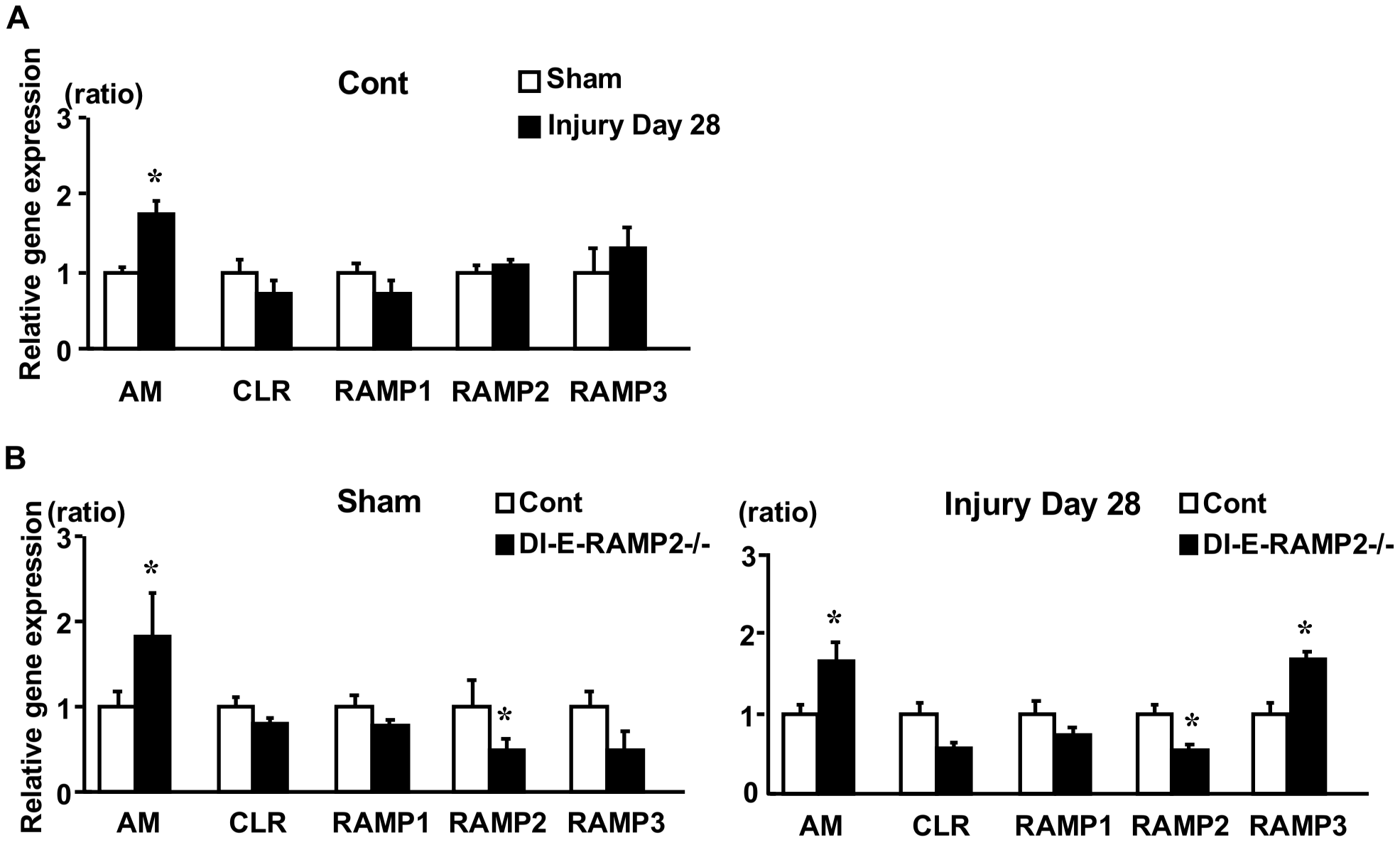
A
Cont
Sham
Injury Day 28
(ratio)
Relative gene expression
3
2
1
0
*
AM
CLR
RAMP1
RAMP2
RAMP3
B
Sham
Cont
DI-E-RAMP2-/-
(ratio)
Relative gene expression
3
2
1
0
*
*
AM
CLR
RAMP1
RAMP2
RAMP3
Injury Day 28
Cont
DI-E-RAMP2-/-
(ratio)
3
2
1
0
*
*
*
AM
CLR
RAMP1
RAMP2
RAMP3

Fig. 4

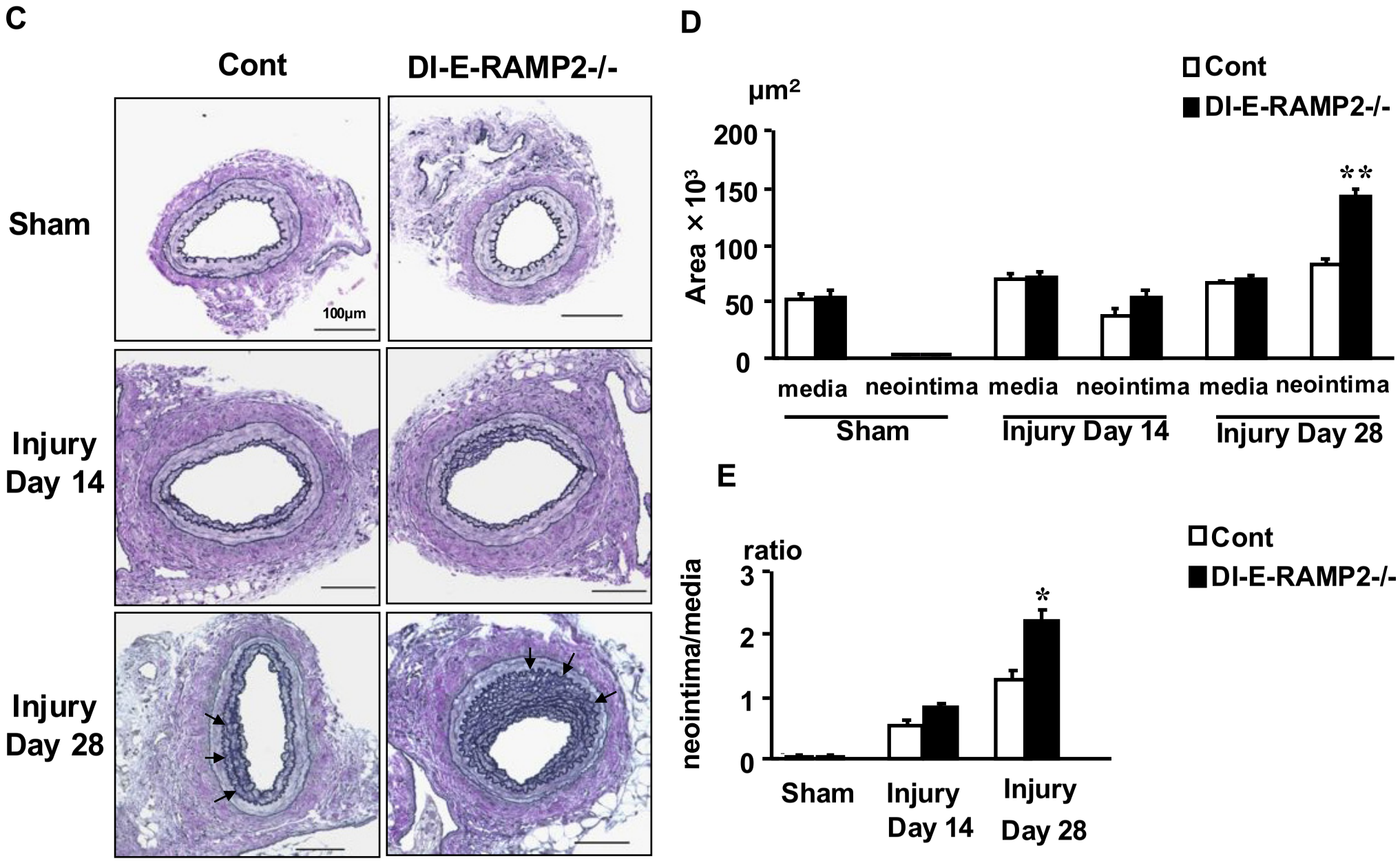
C
Cont
DI-E-RAMP2-/-
Sham
Injury Day 14
Injury Day 28
100μm
D
μm²
Area × 10³
200
150
100
50
0
Cont
DI-E-RAMP2-/-
**
media
neointima
media
neointima
media
neointima
Sham
Injury Day 14
Injury Day 28
E
ratio
neointima/media
3
2
1
0
*
Cont
DI-E-RAMP2-/-
Sham
Injury Day 14
Injury Day 28

Fig. 4

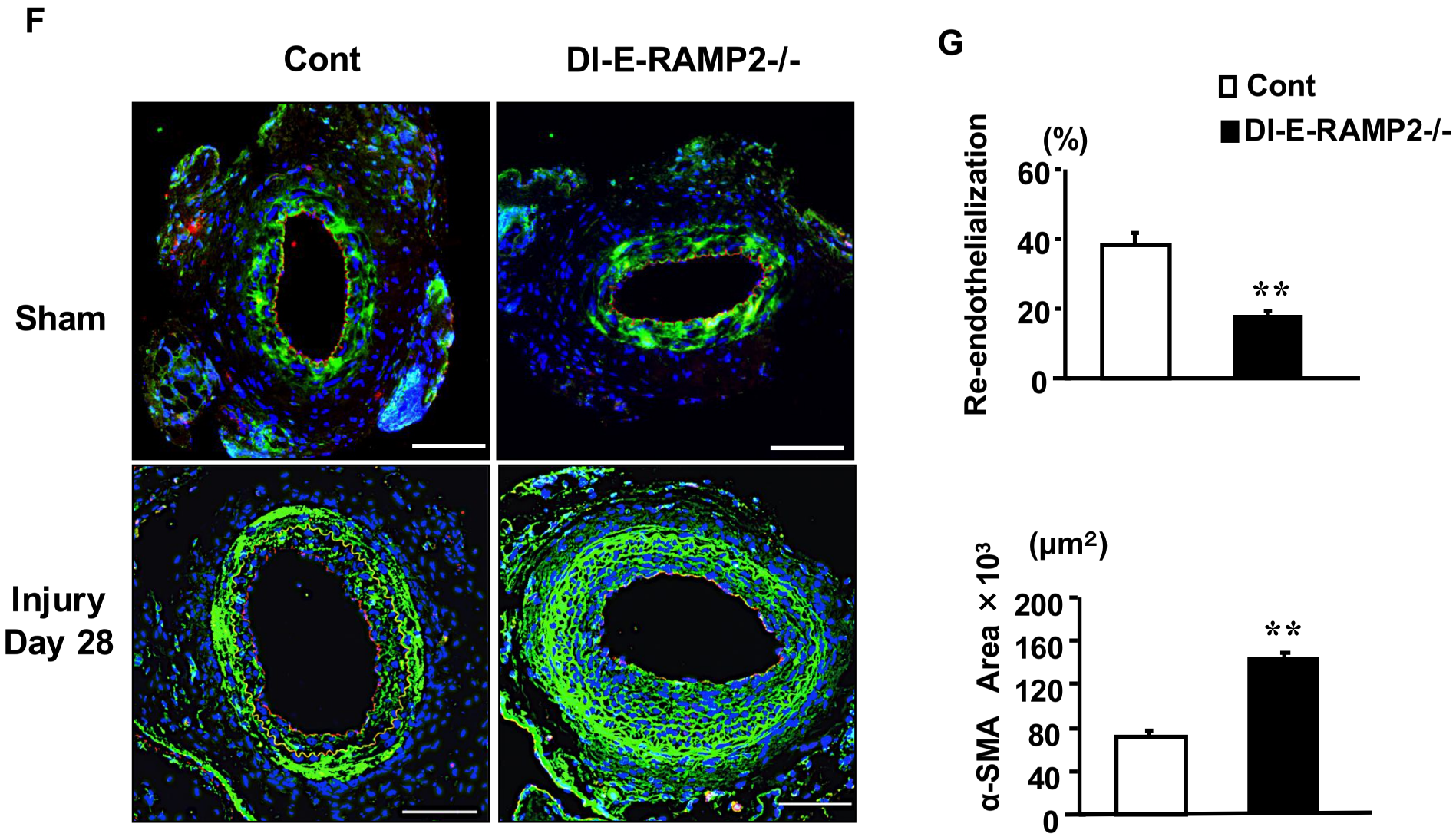
F
Cont
DI-E-RAMP2-/-
Sham
Injury
Day 28
G
Cont
DI-E-RAMP2-/-
Re-endothelialization
(%)
60
40
20
0
**
α-SMA Area × 10³
(μm²)
200
160
120
80
40
0
**

Fig. 4

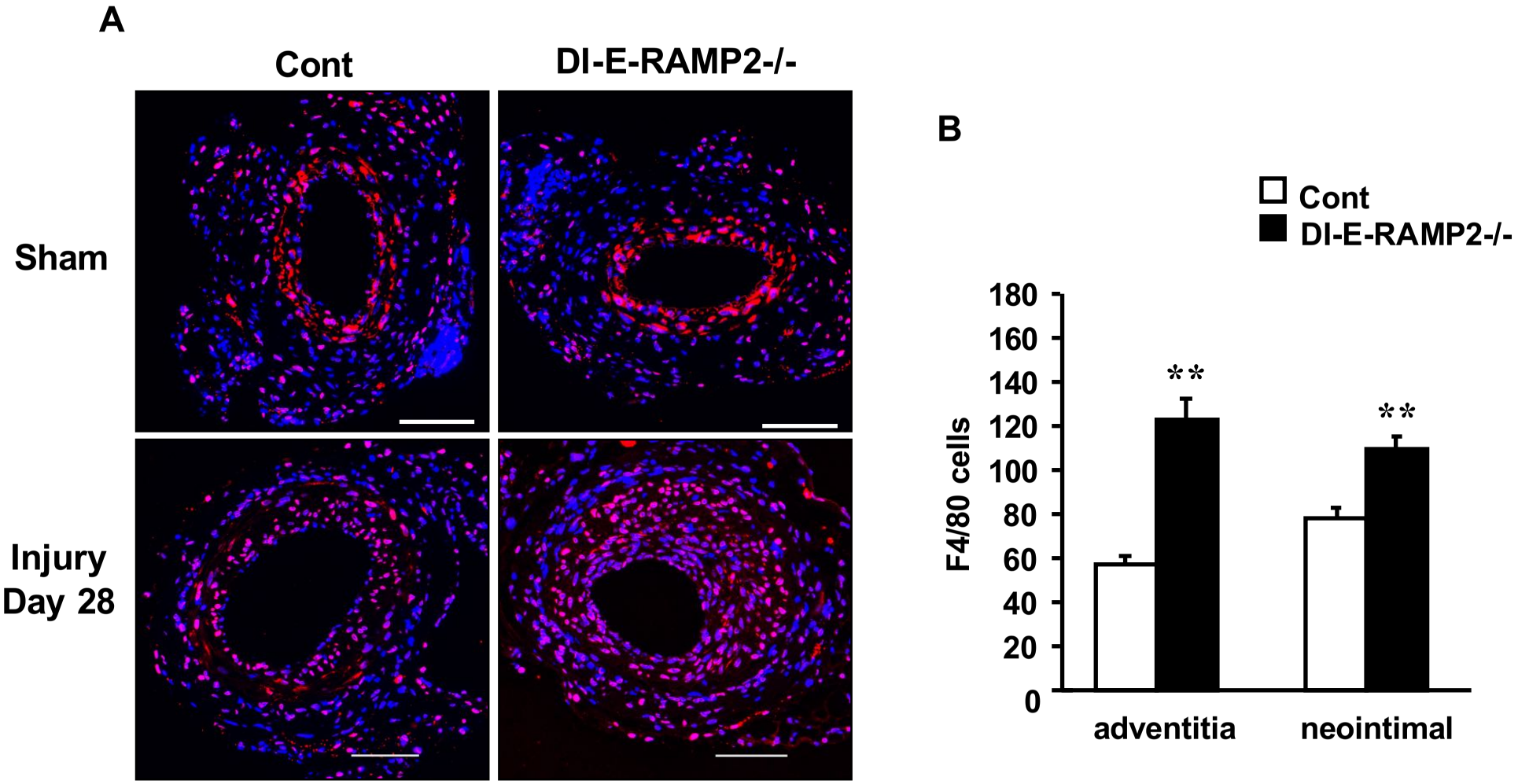
A
Cont
DI-E-RAMP2-/-
Sham
Injury
Day 28
B
Cont
DI-E-RAMP2-/-
F4/80 cells
180
160
140
120
100
80
60
40
20
0
**
**
adventitia
neointimal

Fig. 5

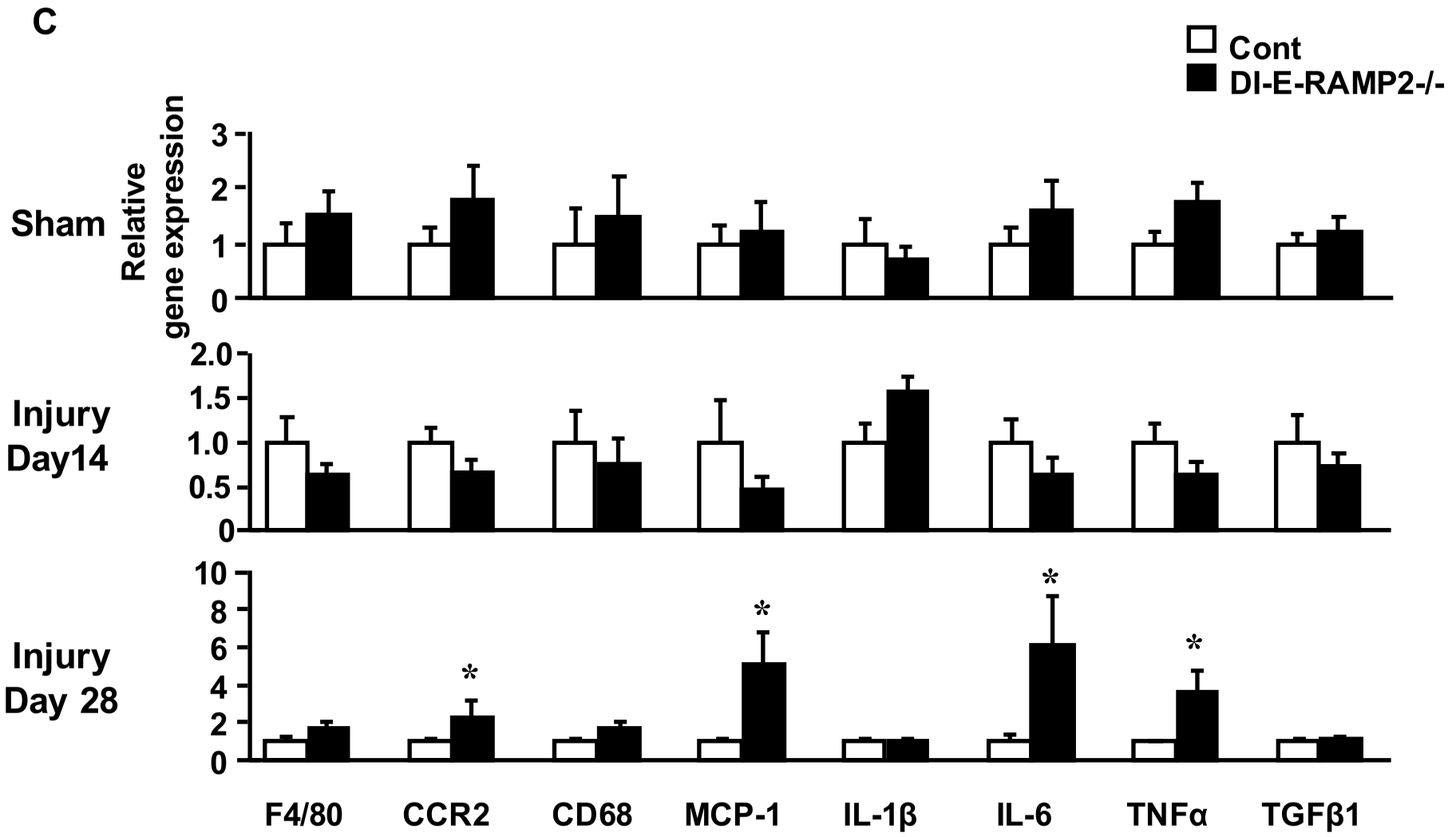
C
Cont
DI-E-RAMP2-/-
Relative gene expression
Sham
Injury Day14
Injury Day 28
3
2
1
0
2.0
1.5
1.0
0.5
0
10
8
6
4
2
0
*
F4/80
CCR2
CD68
MCP-1
IL-1β
IL-6
TNFα
TGFβ1

Fig. 5

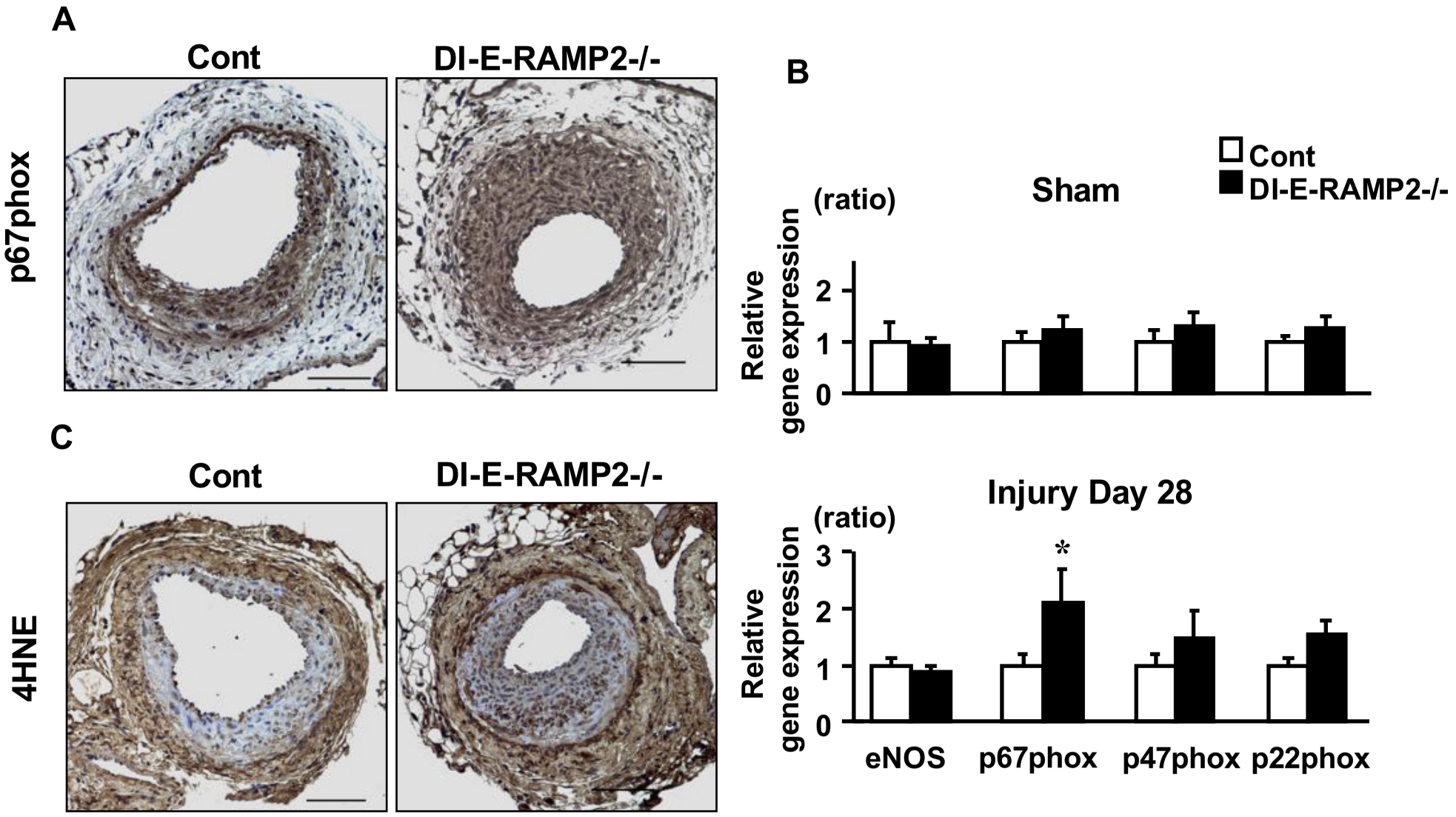
A
Cont
DI-E-RAMP2-/-
p67phox
B
Cont
DI-E-RAMP2-/-
Sham
(ratio)
Relative gene expression
2
1
0
C
Cont
DI-E-RAMP2-/-
4HNE
Injury Day 28
(ratio)
*
3
2
1
0
Relative gene expression
eNOS
p67phox
p47phox
p22phox

Fig. 6

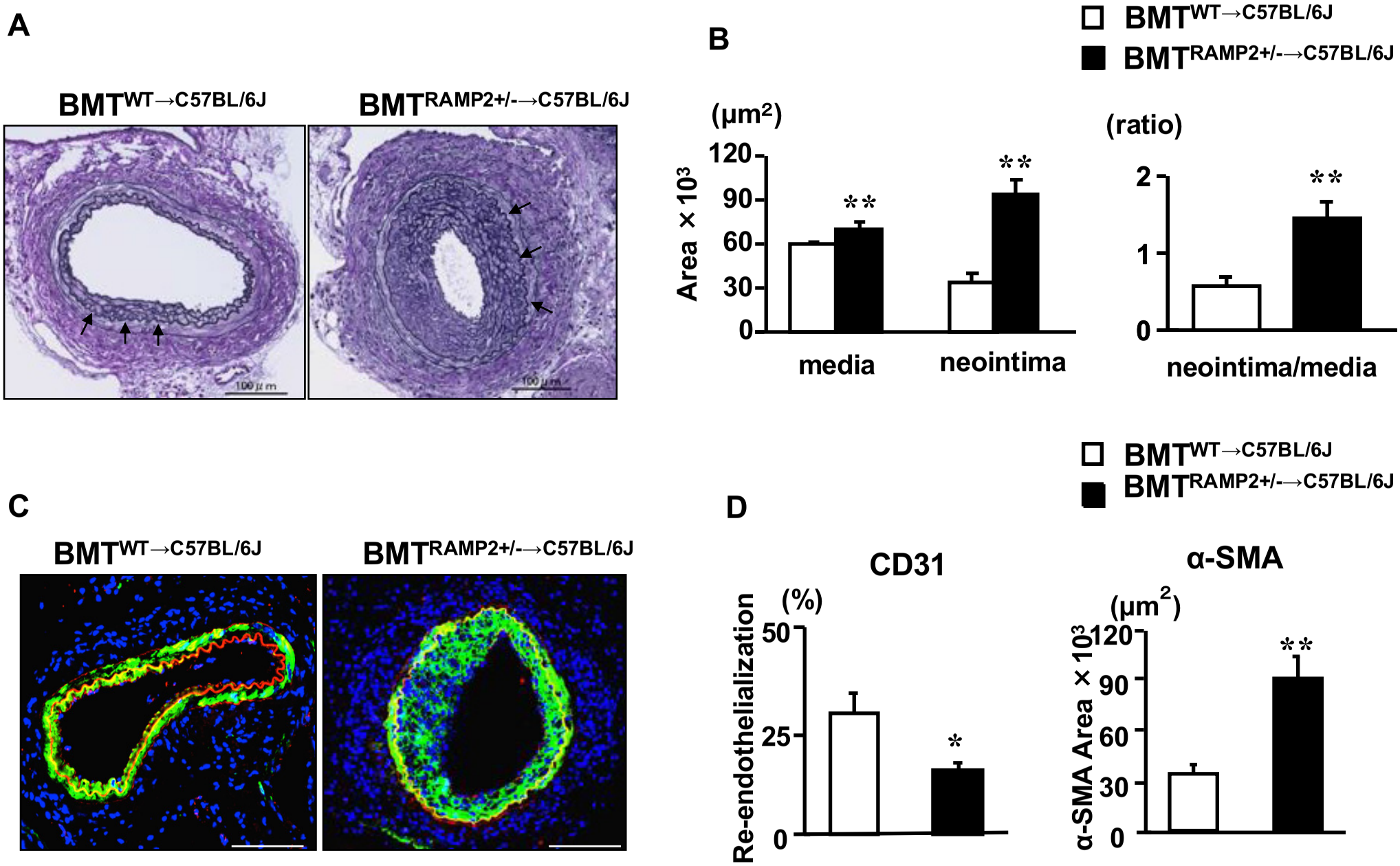
A
BMT^WT→C57BL/6J
BMT^RAMP2+/-→C57BL/6J
100 μm
100 μm
B
BMT^WT→C57BL/6J
BMT^RAMP2+/-→C57BL/6J
(μm²)
Area ×10³
120
90
60
30
0
**
**
media
neointima
(ratio)
2
1
0
**
neointima/media
C
BMT^WT→C57BL/6J
BMT^RAMP2+/-→C57BL/6J
D
BMT^WT→C57BL/6J
BMT^RAMP2+/-→C57BL/6J
CD31
(%)
Re-endothelialization
50
25
0
*
α-SMA
(μm²)
α-SMA Area ×10³
120
90
60
30
0
**

Fig. 7

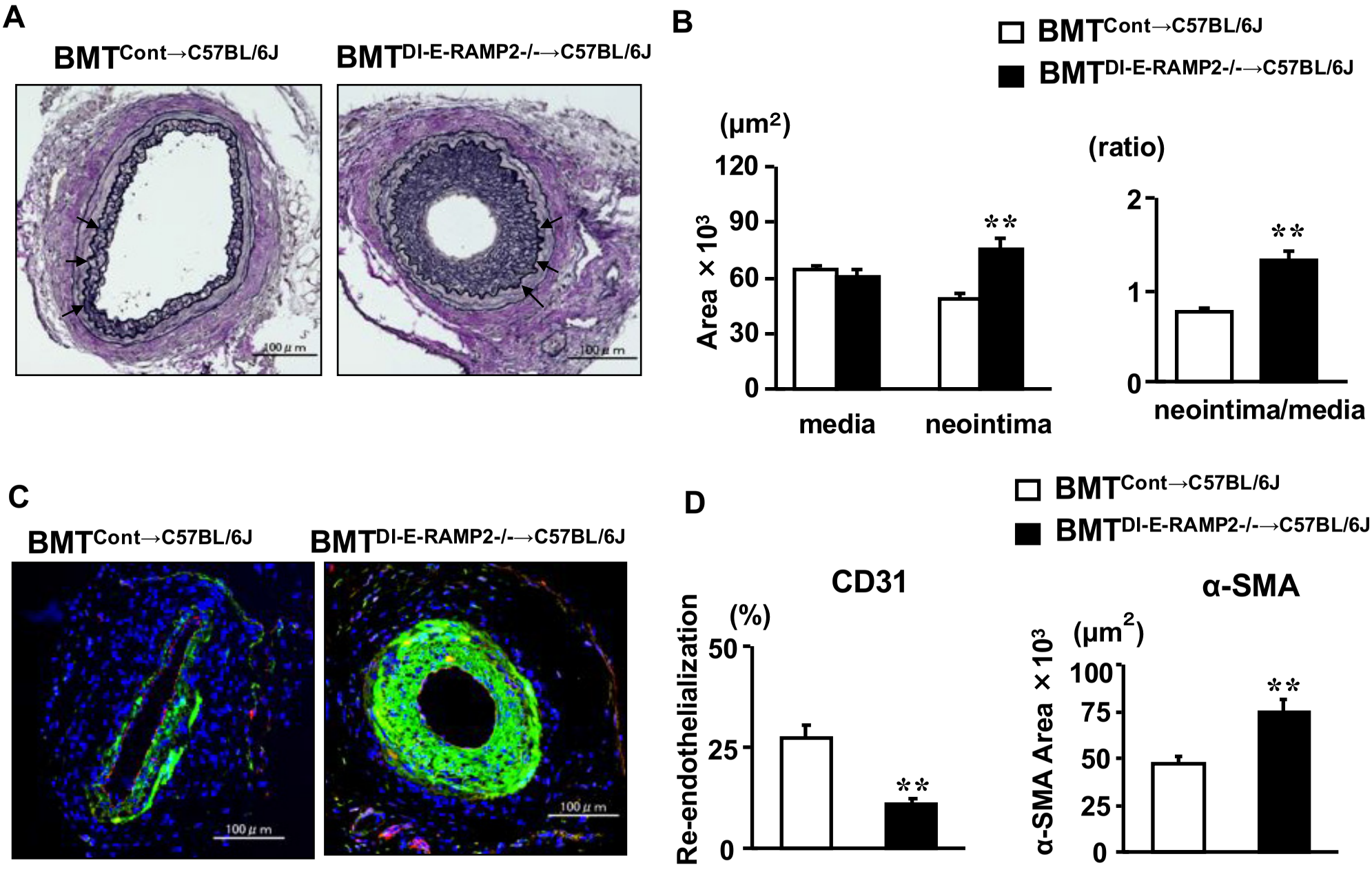
A
BMTCont→C57BL/6J
BMTDI-E-RAMP2-/-→C57BL/6J
100 μm
100 μm
B
BMTCont→C57BL/6J
BMTDI-E-RAMP2-/-→C57BL/6J
(μm2)
Area × 10³
120
90
60
30
0
**
media
neointima
(ratio)
2
1
0
**
neointima/media
C
BMTCont→C57BL/6J
BMTDI-E-RAMP2-/-→C57BL/6J
100 μm
100 μm
D
BMTCont→C57BL/6J
BMTDI-E-RAMP2-/-→C57BL/6J
CD31
(%)
Re-endothelialization
50
25
0
**
α-SMA
(μm2)
α-SMA Area × 10³
100
75
50
25
0
**

Fig. 8

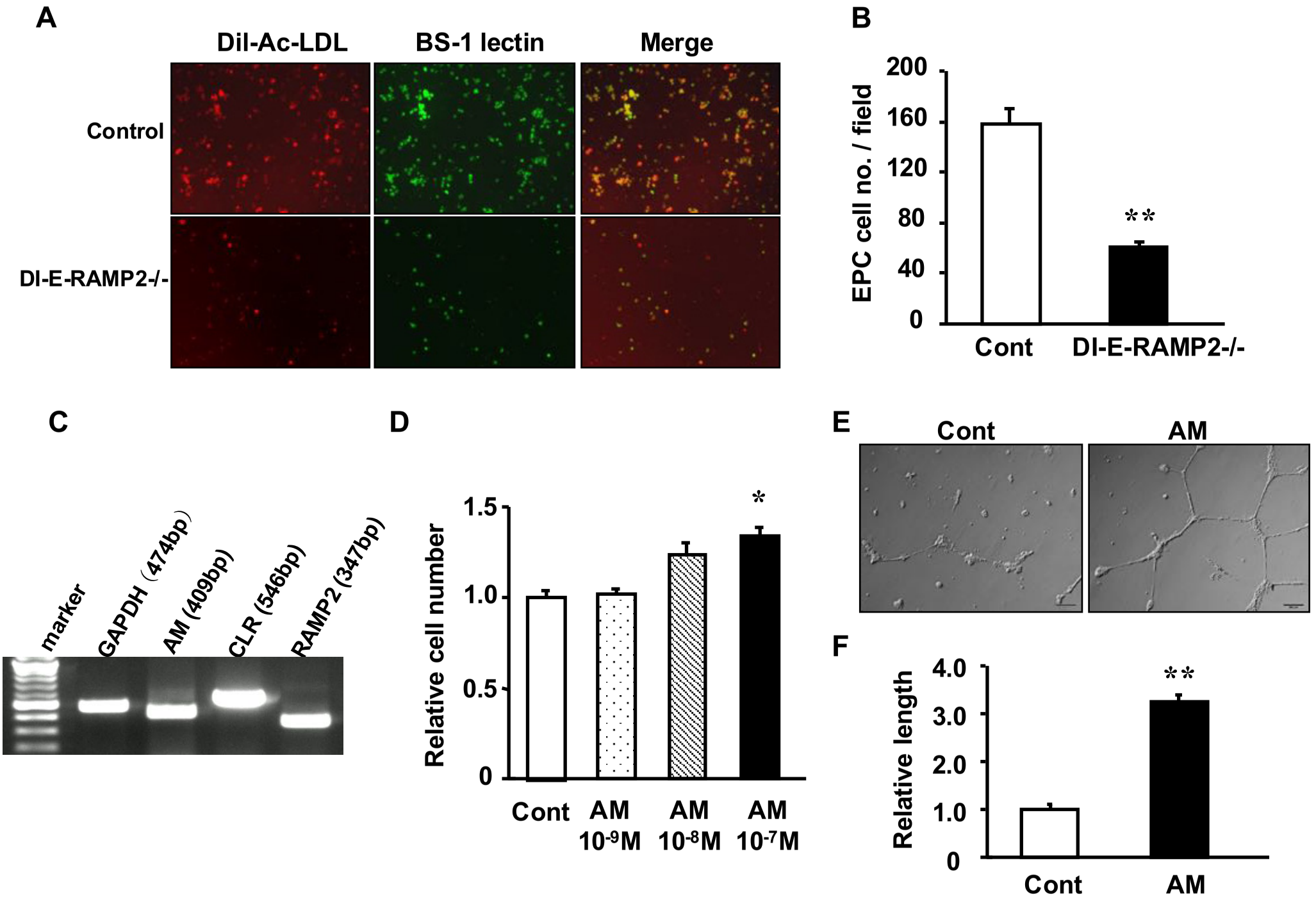
A
DiI-Ac-LDL
BS-1 lectin
Merge
Control
DI-E-RAMP2-/-
B
EPC cell no. / field
200
160
120
80
40
0
**
Cont
DI-E-RAMP2-/-
C
marker
GAPDH (474bp)
AM (409bp)
CLR (546bp)
RAMP2 (347bp)
D
Relative cell number
1.5
1.0
0.5
0
*
Cont
AM 10-9M
AM 10-8M
AM 10-7M
E
Cont
AM
F
Relative length
4.0
3.0
2.0
1.0
0
**
Cont
AM

Fig. 9

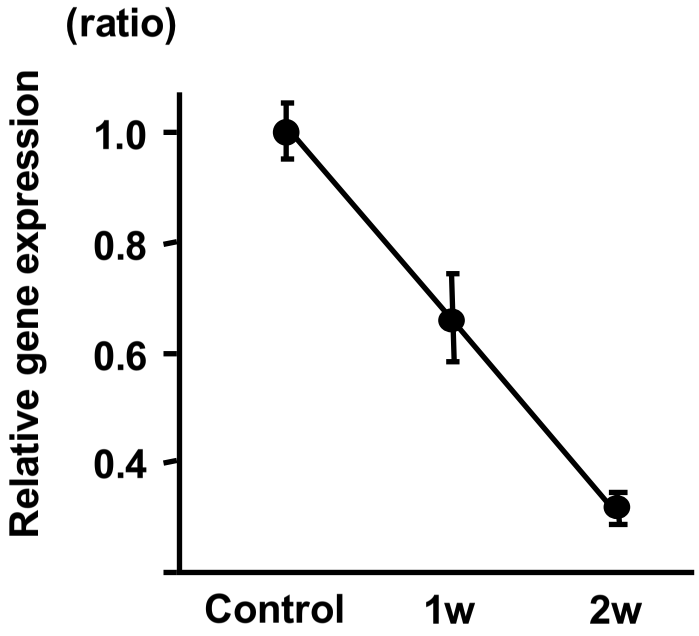

Supplementary Figure 1

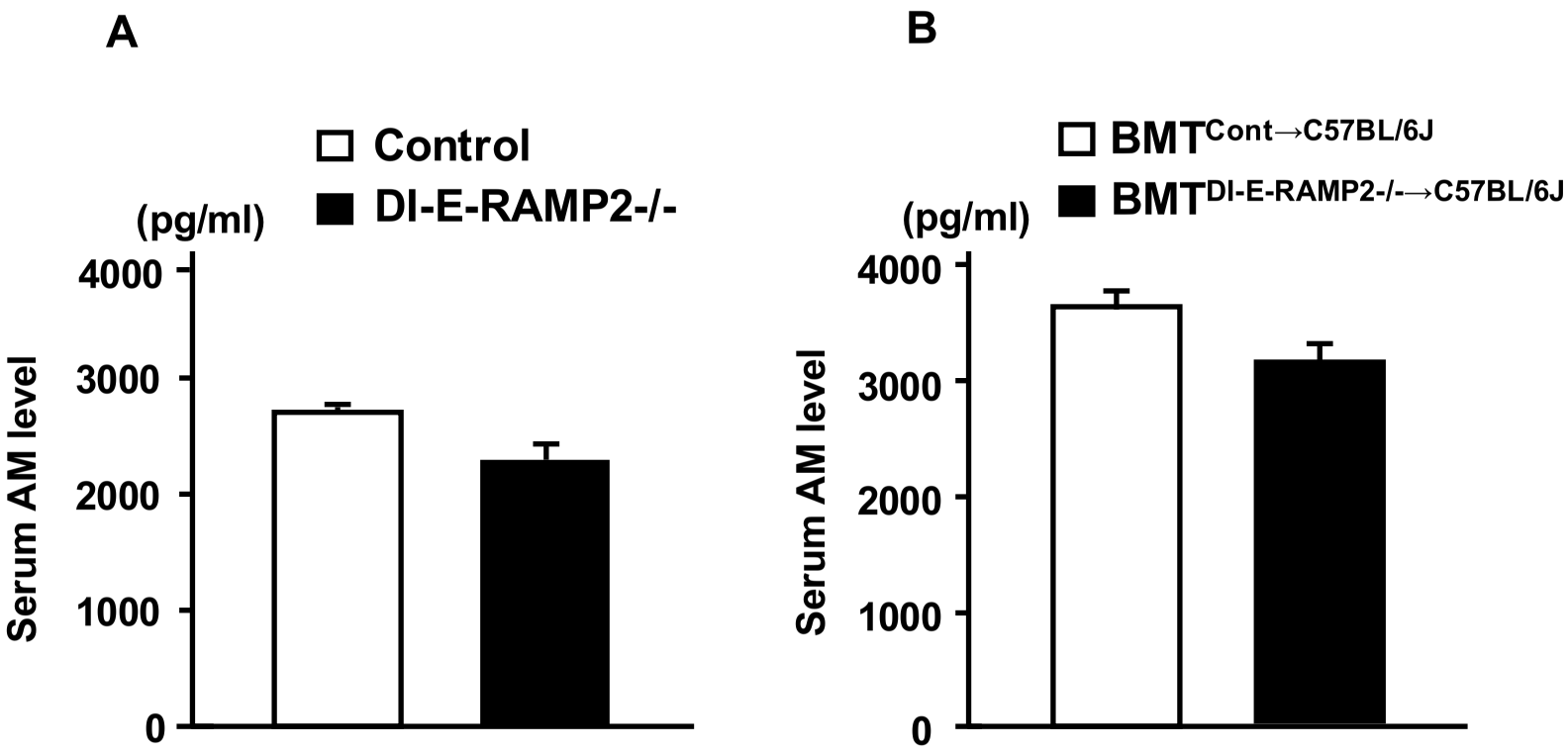

Supplementary Figure 2

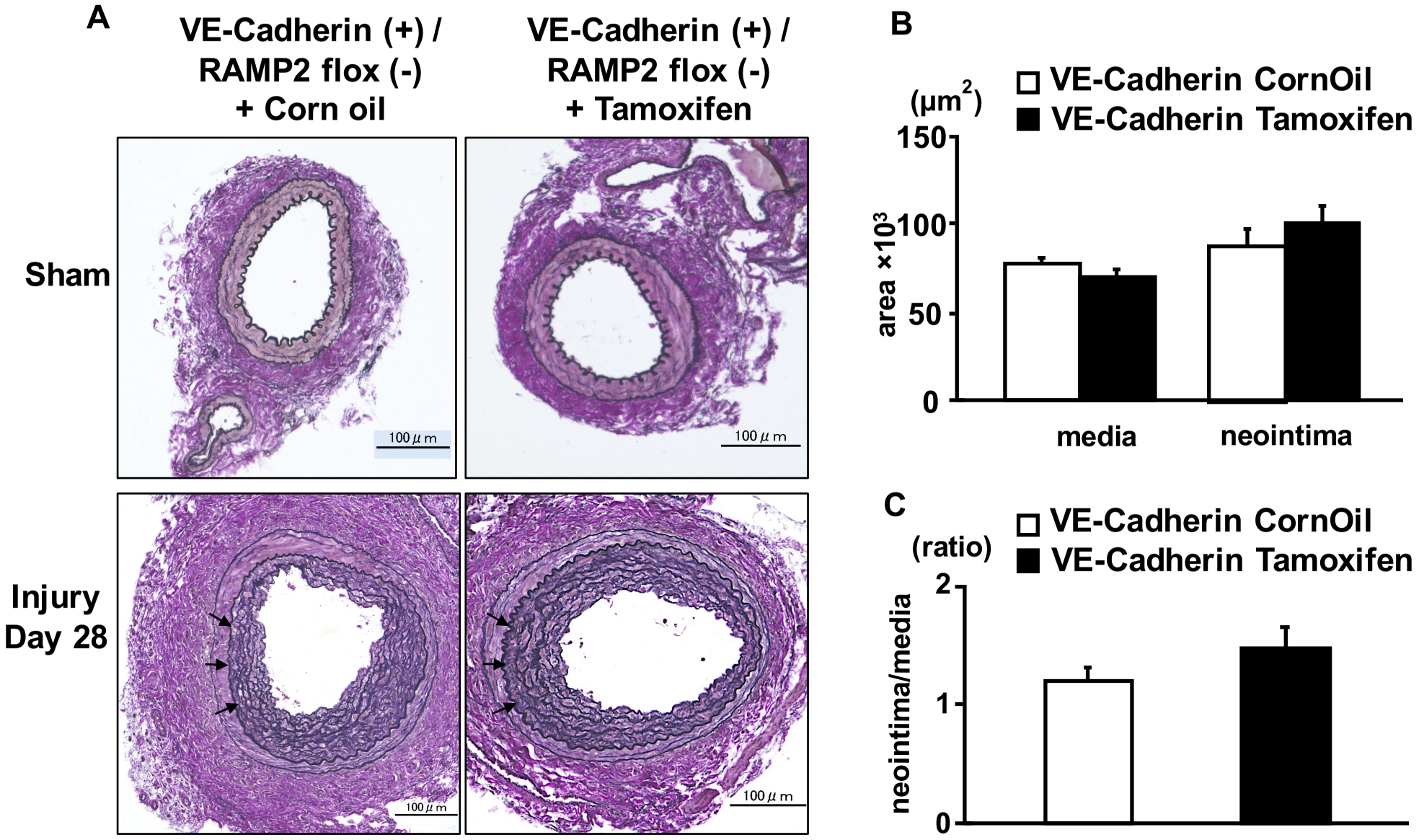

Supplementary Figure 3

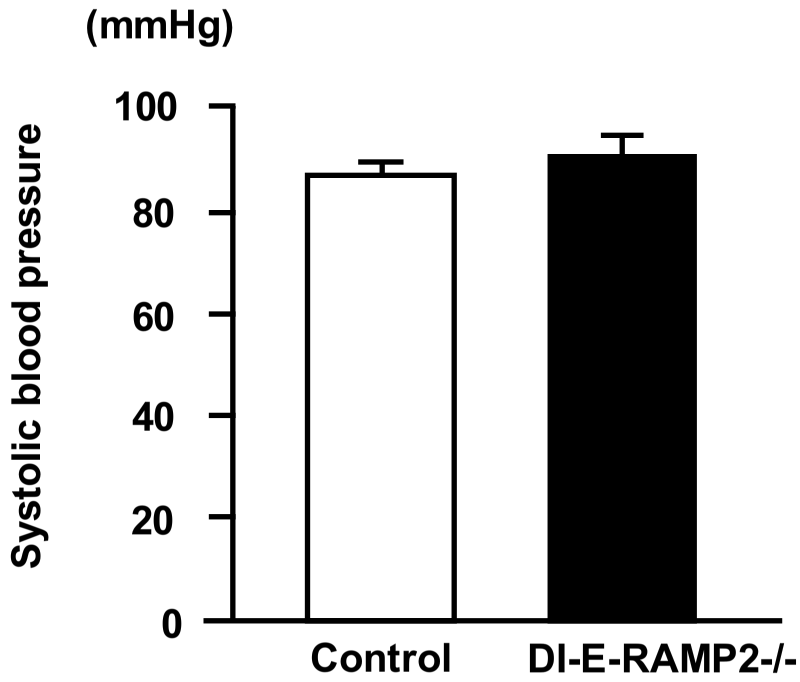

Supplementary Figure 4

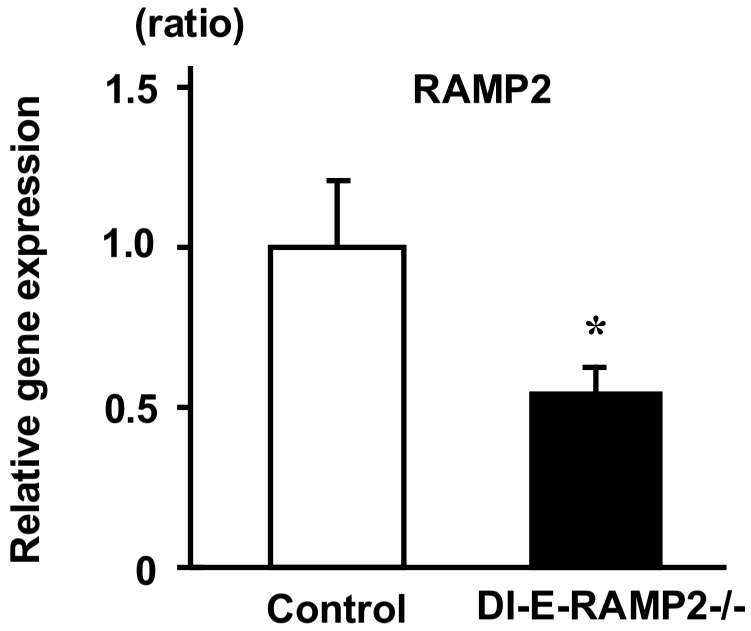

Supplementary Figure 5

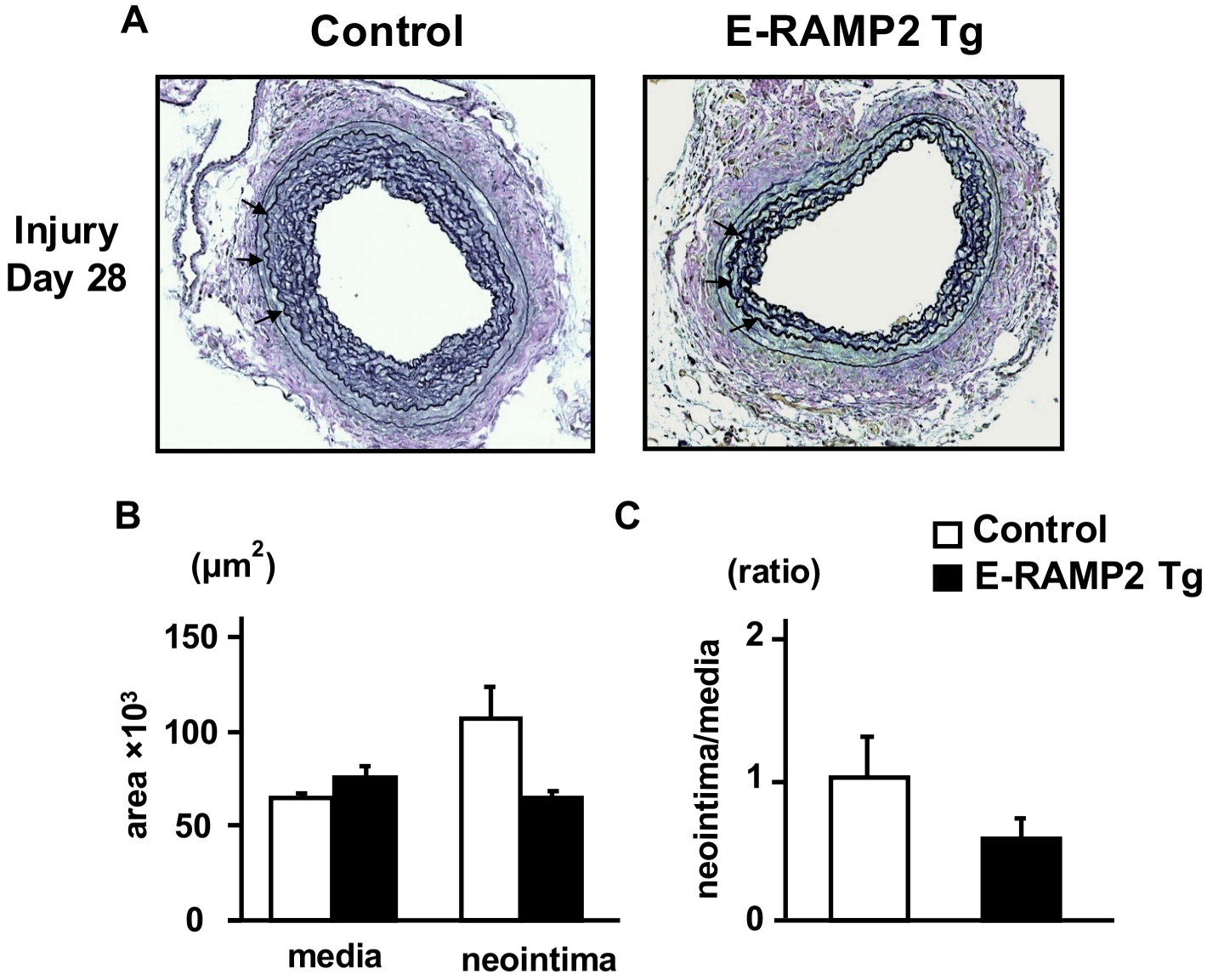

Supplementary Figure 6